Published in final edited form as:
Electrophoresis. 2010 August ; 31(15): 2469–2486. doi:10.1002/elps.201000203.

Recent Developments in Instrumentation for Capillary Electrophoresis and Microchip-Capillary Electrophoresis

Jessica L. Felhofer[a], **Lucas Blanes**[b], and **Carlos D. Garcia**[a,*]

[a] Department of Chemistry, The University of Texas at San Antonio, One UTSA Circle, San Antonio, TX 78249, United States of America

[b] Centre for Forensic Science, University of Technology, Sydney, PO Box 123, Broadway, NSW 2007, Australia

Abstract

Over the last years there has been an explosion in the number of developments and applications of capillary electrophoresis (CE) and microchip-CE. In part, this growth has been the direct consequence of recent developments in instrumentation associated with CE. This review, which is focused on contributions published in the last five years, is intended to complement the papers presented in this special issue dedicated to Instrumentation and to provide an overview on the general trend and some of the most remarkable developments published in the areas of high voltage power supplies, detectors, auxiliary components, and compact systems. It also includes few examples of alternative uses of and modifications to traditional CE instruments.

1- Introduction

Due to increasing demands at the industrial and military levels, there has been a recent trend towards the development of miniaturized or portable sensors. Among others, sensors based on optical responses [1,2], surface plasmon resonance [3,4], metal oxide semiconductors [5,6], fluorescence [7], mass spectrometry [8], or surface acoustic waves [9], have been recently reported. Although most of these sensors are able to detect minute amounts of analytes, one common shortcoming is their versatility. In this regard, sensors based on gas chromatography [10,11] and liquid chromatography [12–14] have the potential to quantify a larger number of important analytes in the same sample without modifications of the hardware. In addition to those, capillary electrophoresis-based sensors [15,16] have caught much attention recently. Capillary electrophoresis (CE) is very attractive because it offers high separation efficiency, low cost, fast analysis, and minimal waste generation. An additional advantage of CE is the simplicity of the required instrumentation, which requires no moving parts and therefore can be easily miniaturized. Consequently, CE and microchip-CE (μchip-CE) have the potential to combine most of the advantages of CE (sample handling capabilities, custom design, and portability) and also offer similar analytical performance as standard bench-top instrumentation. Additional advantages of CE-based sensors include the possibility of using a wide variety of well-established separation techniques, performing the analysis with low-consumption of power, and controlling the entire system electronically. Today, CE and μchip-CE devices have become well-accepted, multidimensional analytical platforms in the biomedical, pharmaceutical, environmental, and forensic sciences [17–24]. In part, this growth has been the direct consequence of the recent developments in associated instrumentation. For that reason, and considering the importance of this issue for the CE community, the current

*To whom correspondence should be addressed. Phone: 01 (210) 458-5774, Fax: 01 (210) 458-7428, carlos.garcia@utsa.edu.

contribution is intended to provide an update on the general trend and some of the most remarkable developments in CE and μchip-CE instrumentation published in the last few years. Reviews specifically describing the development and application of different pumping techniques [25], valves [26], mixers [27], optical sensing systems [28], detectors [29], and different aspects of lab-on-a-chip devices [30,31] have been also recently published. It is worth highlighting two comprehensive reviews focused on portable (non-chip) capillary electrophoresis systems [32] and the state-of-the-art of fully integrated microfluidic separations systems for biochemical analysis [33].

2- Instrumentation

2A- High-Voltage Power Supplies

CE encompasses a family of separation techniques driven by an electric potential difference applied across a narrow-bore capillary (< 100 μm) filled with a (typically aqueous) electrolyte solution. When a potential difference is applied across the capillary, bulk flow of the solution is generated by a process referred to as electro-osmotic flow (EOF) [34]. Analytes, introduced at one extreme of the capillary, are driven toward the detector with a velocity that is proportional to the EOF and their charge/mass ratio. Clearly the use of reliable high voltage power supplies (HVPS) is crucial to perform both separations and electrokinetic injection. Glassman (http://www.glassmanhv.com/) [35] as well as other companies like Spellman (http://www.spellmanhv.com/) [36,37], UltraVolt (http://www.ultravolt.com/) [38,39], Emco (http://www.emcohighvoltage.com/) [40], VMI (http://www.highvoltagepowersupplies.com/), Matsusada Precision Inc (http://www.matsusada.com/) [41], CE Resources (http://www.ce-resources.com/), and Elektro Automatik (http://www.elektroautomatik.de/) [42] offer a variety of options in terms of technical specifications and have been used in recent publications. Although they lay outside the scope of this review, it is worth mentioning few examples of HVPS published before 2005 [43–49].

Typically, HVPS can apply up to ± 30 kV and ± 300 μA if designed for standard CE, or up to ± 3kV and ± 100 μA DC (direct current) if designed for μchip-CE. Current leaks from HVPS can damage internal electronic circuits and is a classic source of noise. Thus, implementation of hardware and software security switches, light/sound alerts, and adequate mechanical protection are fundamental when working with HVPS. As pointed by Collins *et al.* some years ago, while the advent of microchip devices has made the lab-on-a-chip platform accessible to most researchers, there are only a few published descriptions of HVPS which can be utilized to control these devices [50]. In addition to a miniature electrochemical detector, a HVPS powered by universal serial bus (USB) ports was described by Jiang *et al.* [51]. Two strategies were adopted to ensure its efficient power usage: 1) Only two high-voltage converters (one positive and one negative) and two relays were used for power saving, while keeping the sample plug stable and well-defined and avoiding sample leakage for μchip-CE; and 2) The components and their running modes were designed to avoid power waste. Performance of this USB-based mini-HVPS was demonstrated using sodium fluorescein analyte with μchip-CE/LIF (laser-induced fluorescence) detection. The high-voltage board used in this complex and interesting design was built using the converters EMCO Q15-5 and Q15N-5. The authors described that the output voltages of this module ranged from ±250 to ±1.5 kV at 0.5 W. A versatile programmable eight-path-electrode power supply (PEPS) system for manipulating a complex microfluidic chip was developed using, among other components, two 12-bit digital-to-analog converters (D/A, DAC7614, BB, USA), six amplifiers (LM324, National Semiconductor, USA), eight DC–DC high-voltage modules (DW-P802-1.0D, Tianjin Dongwen Power Supply Factory, China), eight ground switch high-voltage relays (K81C235, Kilovac, Cll Technologies, USA), eight floating switch high-voltage relays (LRL-102-100PCV, Okita, Japan), and one over-current protection relay (943H-1C-3DS,

Shanghai Eighth Radio Factory, China) [52]. As shown Please insert Figure 1, the PEPS and the μchip-CE were connected by six Pt electrodes and coupled with a home-made LIF detector. The voltage output of each of the six electrodes was in the range of 0 to +8000 V (0.1% precision) while the current output was in the range of 0 to +999μA.

Other high voltage sequencers are commercially available, for example at Lab Smith (http://www.labsmith.com/) or Major Science (http://www.major-sci.com.tw/). This option enables the possibility of coupling phase-coordinated sinusoidal and other waveforms to the separation potential.

2B- Detectors

It is clear that one of the most critical aspects of analysis by CE and μchip-CE is the detection. The traditional limitation of sensitivity is, in some cases, exacerbated by minute sample volumes, the presence of the electric field, or the small pathlength available in CE systems. Consequently, new detection strategies are constantly being developed. In order to complement previous reviews addressing the challenges and advantages of specific techniques [28,53,54], this portion will be mainly focused on the instrumentation aspects of the detection devices. It is also worth mentioning a recent review by Li *et al.*, discussing dual detection methods for CE and μchip-CE [55].

Optical Detection—Optical has traditionally been the most commonly used detection method in CE and μchip-CE. Although other zones of the spectra such as the infrared spectral region have been used [56], UV-Vis is the default detection method in most commercial instruments. Pertinent examples include Beckman [57], Shimadzu [58], Waters [59], Hitachi [60], Caliper [61], Agilent [62,63], or Bio-Rad [64], just to name a few. The advantages of UV-Vis detection include versatility (most organic analytes absorb light in this range), speed, and a wide variety of commercial sources. In order to increase the sensitivity in μchip-CE, a three-dimensional U-type flow cell (126 μm pathlength) was microfabricated and evaluated using a green light-emitting diode (LED) (525 nm, Allied Electronics), a microscope objective (Newport, U-27X), a red-shifted photomultiplier tube (PMT) (H5784, Hamamatsu), and LabView (National Instruments, Austin, TX) [65]. Indirect detection (UVIS 200, Linear, Reno, NV) has also been recently applied [66]. Probably due to the extraordinary limits of detection (LODs) and dynamic range [67], most instrumental developments in terms of optical detection have been focused on fluorescence detection. In this regard, authors have used commercial instruments [68] or coupled the capillary with either fluorescence microscopes [69,70] or home-built detectors. Using the latter approach, an inverted fluorescence microscope (CK40, Olympus, Japan), a diode laser (808 nm, 1W, Institute of Semiconductor, Beijing, China) or Ti:Sapphire laser (Spectra Physics, USA), a dichroic mirror (E625SP, Chroma, USA), an oil objective (100×, NA1.25, Olympus, Japan), a PMT (R5070, Hamamatsu, Japan), and a low-pass filter (BG18, Newport, USA) were used to first demonstrate the advantages of continuous wave-based multiphoton excitation fluorescence for CE [71]. Rodat *et al.* utilized an ellipsoidal mirror, glued on the capillary window and screwed inside the capillary cassette, to allow the collection of the fluorescence in the capillary, trapped by a silica/air interface [68]. The performance of this new detector setup was found to be identical to the collinear setup using the same ball lens. Using this setup the LOD of Immunoglobulin G2 was calculated to be in the 50 $pg{\cdot}mL^{-1}$ (tetramethylrhodamine-labeled, 532 nm diode laser, 25 mW, CrystaLaser, Reno, USA) to 150 $pg{\cdot}mL^{-1}$ (fluorescein isothiocyanate-labeled, 488 nm argon ion, 25 mW laser Spectra Physics, Mountain View, CA) range. A new LIF detection system based on a line laser beam for μchip-CE analysis was developed by Xu *et al.* [72]. This detection system was constructed by using a solid-state laser system (488 nm, 20 mW, model: 85BCD-020-230, Melles Griot Inc) as the light source and collecting the fluorescence using objective lens (Rolyn Optics), a 493 nm long-pass filter (Model: XR3000/493AELP, Omega Optical, Inc.), a 530

nm band-pass filter (Model: XCY-530DF30, Omega Optical, Inc.), and a PMT (H9301, Hamamatsu photonics K.K., Electron Tube Center). An in-house program (Visual C++ 6.0, Microsoft Corporation) was used to visualize the data and perform a 30-point adjacent averaging smoothing program. Using FITC (fluorescein isothiocyanate) as a model analyte, authors reported LODs of 0.13 nmol·L^{-1}. A similar system, composed by a 9 mW Ar-ion laser (Spectra Physics, Mountain View, CA, USA), a 40X microscope objective, a 550 nm cut-off filter and an interference filter, and a PMT (R928 Hamamatsu, Masse, France), was used to obtain protein fingerprinting of *Staphylococcus* species by CE with on-capillary derivatization [73]. An on-line wall-free cell for LIF detection was fabricated by etching a 10 mm × 50μm inner diameter (ID) fused-silica capillary [74]. The wall-free cell was mounted on a three-dimensional micropositioner (Zolix Instruments, Beijing, China) to adjust the cell center to the waist of the laser beam. The fluorescence signal was amplified by a GD-1 optical detector (Xi'an Reike Electric Equipment, Shanxi, China) and recorded by an N-2000 double-channel chromatography processor (Institute of Information and Engineering, Zhejiang University, Zhejiang, China). According to the report, significant improvements (6–15 fold when compared with on-column cell) were obtained with the proposed cell. A system featuring a two-laser, two-color detector was also developed and applied for the detection of cytokines (naturally occurring and recombinant) in biological samples [75]. By labeling recombinant cytokines with Bimane (detected at 408 nm) and endogenous cytokines with AlexaFluor633 (detected at 633 nm), Morgan and coworkers were able to obtain two parallel electropherograms. The corresponding overlaid traces enabled quantification of the endogenous cytokines with excellent recoveries. Instead of using the conventional LIF setup equipped with delicate spatial filters and complex control systems, Lin *et al*. proposed the use of a hollow cone illumination generated using a dark-field condenser (Dry 0.95–0.80, Nikon) to converge light from a 20 W tungsten bulb [76]. Other parts of the system include a UV–Vis–NIR spectrophotometer (HR4000, Ocean Optics, Dunedin, FL, USA), a multimode fused-silica fiber (P400-2-UV/Vis, Ocean Optic), and a programmable HVPS (MP-3500, Major Science, Taipei, Taiwan). Although the LOD (5 μmol·L^{-1}, FITC) is not extraordinary, experimental results show that the proposed system is feasible for simultaneously detecting a mixed sample composed of three fluorescent dyes (Atto 610, Rhodamine B, and FITC) in a single run. Furthermore, a mixed sample composed of two 16-mer single-stranded deoxyribonucleic acid (DNA) molecules (labeled with Cy3 and FITC) was also successfully detected with the proposed system. The same group later presented an advanced diascopic illumination technique for simultaneous multi-wavelength fluorescence excitation and detection without using any spatial filter sets [77]. This system enabled the separation and detection of a sample composed of three single-stranded DNA samples labeled with Cy3, FITC, and Alexa647 fluorescence in a single channel. The impact of the excitation intensity of a deep-UV laser (266 nm continuous wave) on the signal-to-noise ratio (S/N ratio) of aromatic compounds as well as of proteins was also investigated [78]. Although LODs in the 113 – 475 nmol L^{-1} range (for serotonin and 3-phenoxy-1,2-propandiol, respectively) were achieved, fluorescence saturation and photobleaching effects were observed.

In order to overcome the limited flexibility of traditional LIF systems (due to the limited number of excitation lasers and low detection frequencies), a xenon lamp (75 W, U-LH75XEAPO, Olympus), a fluorescence microscope (IX-71S1F, Olympus), a spectrograph with exchangeable gratings (150 and 600 lines/mm) and an intensified charge-coupled device (CCD) camera (PI-Max 512RB, Princeton Instruments) were used by Gotz and Karst [79]. The proposed approach enabled the whole visible spectrum of light (350–800 nm) to be used for excitation and emission and to record on-line emission spectra with high repetition rates (up to 60 Hz), which are needed to monitor rapid on-chip separations with peak widths <0.5 s. The performance of the system was demonstrated by performing μchip-CE separation of three rhodamines and their impurities (excitation: 450–490 nm; emission: >500 nm) at sub-μmol·L^{-1} concentrations.

One of the current trends in optical detection is to move away from expensive lasers and use LEDs as light sources. The combination of high stability, small size, low cost, and very long lifetime make LEDs an very attractive excitation source for fluorescence detection, especially to design miniaturized or portable devices [80,81]. Using this approach, Arraez-Roman and coworkers constructed a simple fluorescence detector for both direct and indirect CE methods using a blue LED (470 nm, LED-470, Ocean Optics) as excitation source, a bifurcated optical fiber as a waveguide, and a CCD camera as a detector [82]. According to the report, the connection of all the components is fairly easy (even for non-experts) and the use of a CCD camera improves the applicability of this detector compared to the others using PMTs because it permits the recording of two-dimensional electropherograms or phosphorescence measurements with LODs in the low $\mu mol \cdot L^{-1}$ range. Using a LED (with enhanced emission spectrum, 150 mA × 3.05 V, Shifeng Corp., China), a band pass filter (BP 470 nm, FWHM 30 nm, Huibo Optical Corp. Ltd., China) as the excitation light source, and a metal-packaged mini-PMT (H5784, Hamamatsu, Japan), Xu *et al.* constructed and evaluated the performance of a fluorescence detector for CE applications [83]. This arrangement and the use of a refractive index (RI)-matching fluid enabled reducing scattering light and the noise level to reach a LOD of 1.5 $nmol \cdot L^{-1}$ (fluorescein). The combination of a blue LED (473 nm, ZD 0180, Jaycar) and a highly absorbing (478 nm) anionic dye (Orange G, dissolved in methanol to reduce adsorption to the capillary wall) were used to perform indirect photometric detection of inorganic and organic anions [84]. In this report, a range of commercial LEDs was tested to improve the detection performance, with a difference of 25% in sensitivity being observed between the best and worst performing LED. The optimized background electrolyte (4 $mmol \cdot L^{-1}$ Orange G, 0.05% w/v hydroxypropylcellulose, 20 $mmol \cdot L^{-1}$ triethanolamine, in methanol) exhibited stable baselines and enabled two- to six-fold improvement in LODs (over previous studies). Segura-Carretero *et al.* described the performance of a homemade, simple, LIF detector for CE [85]. Combining an LED as excitation source, a bifurcated optical fiber as a waveguide, and a CCD as a photodetector this device provides a low-cost and rapid alternative for the determination of high-quantum-yield native fluorescence compounds (R-phycoerythrin and B-phycoerythrin) as well as compounds labeled with FITC. Detection limits in the low $\mu mol \cdot L^{-1}$ range were achieved. One of the cheapest (less than $50) alternatives to perform fluorescence detection was described by Yang *et al.* [86]. In this work, a blue concave LED (excitation source), a lens (obtained from a broken DVD-ROM), an ocular (obtained from a pen microscope), a band-pass filter, and a photodiode detector were used. The performance of this detector was demonstrated in CE separations using sodium fluorescein and FITC-labeled amino acids as model samples, reaching LODs of 0.92 $\mu mol \cdot L^{-1}$. Krmová *et al.* investigated the suitability of a deep-UV LED (Seoul Optodevice 255 nm from Sensor Electronic Technology, Columbia, SC, USA,) as a novel light source for photometric detection [87]. Although the use of this LED (see Please insert Figure 2) enables the detection of nucleotides with satisfactory performance and LODs in the $\mu mol \cdot L^{-1}$ range (for adenosine monophosphate, adenosine diphosphate, and guanosine diphosphate), authors also found that the emission spectrum deep-UV-LED contains significant parasitic emission bands in the 400–500 nm spectral region.

A novel miniaturized and multiplexed, on-capillary, RI detector using liquid core optical ring resonators (LCORRs) was also developed [88]. The LCORR employs a glass capillary with a diameter of 100 μm and a wall thickness of a few micrometers. The circular cross section of the capillary forms a ring resonator along which the light circulates in the form of the whispering gallery modes (WGMs). The WGM has an evanescent field extending into the capillary core and responds to the RI change due to the analyte conducted in the capillary, thus permitting label-free measurement. The resonating nature of the WGM enables repetitive light analyte interaction, significantly enhancing the LCORR sensitivity. This LCORR architecture achieves dual use of the capillary as a sensor head and a CE fluidic channel, allowing for integrated, and multiplexed on-capillary detection at any location along the capillary. In this

work, EOF and glycerol were used as a model system to demonstrate the fluid transport capability of the LCORRs. In addition, a flow speed measurement was performed on the LCORR to demonstrate its flow analysis capability. Finally, using the LCORR's label-free sensing mechanism, the analyte concentration was deduced in real time at a given point on the capillary. A sensitivity of 20 nm/RIU (refractive index units) was observed, leading to an RI detection limit of 10-6 RIU. The LCORR marries photonic technology with microfluidics and enables rapid on-capillary sample analysis and flow profile monitoring [88]. In order to demonstrate the advantages of combining organic LEDs, Si:H based multispectral photodiodes as detectors, and monolithic integration, Merfort *et al.*, adapted the spectral response of a tunable multispectral photodiode to individual fluorescence spectra of different dyes [89]. The organic LEDs used in the report were fabricated using PDY-132 thin-films (<1 μm) that emit in the green region of the visible spectrum and had active areas of in the 0.9 to 2.1 mm^2 range.

A highly sensitive chemiluminescence detection system was also developed for detection of enkephalin-related peptides labeled with acridinium ester [90]. The interface included two sections to 1) acidify the capillary outflow (so that the corresponding acridinium pseudo-base form can be changed into acridinium ester form by adding excess acid to the system), and 2) provide a suitable solution to produce the chemiluminescence from acridinium ester. This allowed reaching detection limits in the attomole range. A system using CE/$Ru(bpy)_3^{2+}$ electrochemiluminescence detection with the assistance of ionic liquids was also recently presented [91]. Although not strictly instrumental, an analytical method to calculate radiative fluxes incident on a planar circular detector from a volume multiple point chemi- or bio-luminescent source inside a coaxial cylindrical reactor was proposed [92]. The obtained formulas are suitable for optimizing and/or calibrating the considered source-detectors systems (optical radiometers or luminometers) and determining radiative fluxes generated by chemical, biological, and physical processes. According to Mandaji *et al.* the performance of fluorescence detectors in CE can be maximized by modulating the excitation light intensity [93]. In such case, the PMT-amplified raw output signal can be captured directly by a personal computer sound card and processed by a lock-in emulated by software. The LODs obtained were at least three times better compared to conventional systems based on LEDs.

Electrochemical Detection—The cost of classic optical instrumentation, the frequent need for analyte derivatization, and the limited portability of LIF have led to a significant interest in electrochemical detection (ECD) as an attractive alternative for detection in CE and μchip-CE. As one of the first examples of an ECD designed for CE, Martin *et al.* presented an isolated potentiostat that enabled placing the working electrode directly in the separation channel, avoiding the use of a decoupler [94]. The potentiostat had several components of a conventional 3-electrode digital potentiostat: analog-to-digital converters (ADC), digital-to-analog converters, voltage reference, timer, digital control, serial communication, and nonvolatile memory. Different modes of ECD [95,96] can be used with many different assay types, offering remarkable mass sensitivity (approaching that of fluorescence), inherent miniaturization of both the detector and control instrumentation, independence from sample turbidity and substrate clarity, low cost, minimal power demands, and high compatibility with advanced micromachining and microfabrication technologies [97,98]. Moreover, the analytical sensitivity is not compromised by miniaturization, the associated instrumentation is relatively simple (compared to optical detectors or mass spectrometry), and electrodes for detection can be fabricated with different materials, allowing significant improvements in sensitivity and selectivity [99]. Despite these advantages, two main challenges still affect the widespread use of ECD: 1) a limited number of commercial ECDs are available [100] and 2) (probably most importantly) there is the need to eliminate the effect of the strong electric field used in electrophoretic separation from the conditions of electrochemical detections [101]. With respect to the first point, commercial instruments from Metrohm (Switzerland), ECO Chemie (Netherlands) [102], CH Instruments (Austin, TX) [103–106], Bioanalytical Systems (West

Lafayette, IN) [107], Palm Instruments BV (Netherlands) [108], Pinnacle Tech. (Lawrence, KS) [109], or ESA Biosciences (Chelmsford, MA) have been used in conjunction with CE. In order to minimize the effect of the separation potential the three main approaches [96,110] have been proposed: placing the detection electrode aligned just outside the separation channel (end-channel) [111,112], placing the detection electrode in the separation channel (in-channel, requires using an isolated potentiostat) [113], and using a decoupler to ground the separation voltage before it reaches the detector, typically made with Pd (off-channel) [114,115]. As relevant examples of the latter approach, Scott Martin's group has investigated several designs of decouplers and found that the optimal distance between the first electrode and the decoupler was 250 μm, while the distance between the two electrodes has been optimized at 100 μm [116,117]. Alternatively, a μchip-CE containing an integrated sheath-flow ECD was developed. The microdevice consists of an upper glass wafer (carrying the etched separation, injection, and sheath-flow channels) and a lower glass wafer (with the Au and Ag electrodes) [118]. The same principle was later used to develop an ECD system capable of accommodating capillaries with ID larger than 25 μm [119]. In line with this, a general literature search shows that most of the work in this area has been directed to the design and integration of the detection electrodes with the separation channel [118,120]. In this regard, a homemade on-column ECD cell and pressure program was employed to perform two-dimensional CE coupled with on-column ECD [121]. Just to name a few examples at the microchip scale, Joo *et al.* used evaporation to deposit Au electrodes (250 μm width, 320 nm thick) on a glass substrate coated with an adhesion layer of Ti (50 nm) [122]. Using a permanent dry film resist (Ordyl SY300) to create microfluidic channels (followed by electroplating of silver and subsequent chlorination) a full-wafer process was presented for fast (1 day) and simple fabrication of glass microfluidic chips with integrated electroplated electrodes [123].

In 2007, a mini-ECD for μchip-CE was presented by Jiang *et al.* [51]. The main electrical components of the system were USB to UART BRIDGE CP2101 (from Silicon Laboratories, Austin, TX), a 8-bit microcontroller (MSC1211Y5 with a 24 MHz system clock), an operational amplifier (OPA129, Texas Instruments Inc., Dallas, TX), and a DC–DC converter (ADM660, Analog Devices Inc., Norwood). The electronic diagram of the electrochemical detector is also included in the report. To improve the S/N ratio (<1 pA), low-pass filters were placed at both the input end and the output end in the OPA129 circuit and the OPA129 input pad was designed as short as possible and shielded with ground pads. The analytical performance of the new system was demonstrated by the detection of epinephrine using an integrated (polydimethyl)siloxane (PDMS)/glass microchip reaching a detection limit of 2.1 $\mu mol \cdot L^{-1}$.

A new detector based on the principle of electromagnetic induction for application to CE and μchip-CE has been described [124]. The detector has an inductor connected in series to a high-frequency (optimal frequency 1.63 MHz-1.1 MHz) signal generator. The detection is based on the measurement of the change in inductive reactance (detected by a high-frequency voltmeter and enhanced by an amplifier) produced by the analytes. According to Chen *et al.*, this new detection technique offers simple construction, assembly and operation, and has great potential for universal application. Although not integrated with CE separations, other ECDs have been also described [125–127].

Conductivity Detection—In 1980 Gas *et al.* introduced a first approach for what today is known as capacitively-coupled contactless conductivity detection (C^4D) as a new detection mode applied to isotachophoresis of small ions [128]. Almost two decades later, da Silva and do Lago [35] and Zemann [129] independently published simplified versions of C^4D applied to CE. Since then, the use of CE-C^4D has grown exponentially and is used today for the analysis of small ions as well as complex biochemical species. C^4D is composed of two radial electrodes placed around the capillary or two planar electrodes placed in the end of the microchip channel.

A high-frequency is applied to one of the electrodes and the resulting alternating current that passes through the cell to the second electrode is electronically amplified, rectified, filtered, and converted to a digital signal using an ADC. The positioning of the electrodes outside the capillary simplifies the construction and implementation of this detector. As the electrodes are not in contact with the solution, the high DC electromigration voltages are uncoupled from the low voltage circuit of the detector [130]. In 2005, Brito-Neto *et al.*[131,132], using simulated and experimental results, suggested several aspects to be considered in the development of new detectors or when planning experiments using C^4D. In summary, C^4D sensitivity depends on: 1) analytes and background electrolyte conductivity differences; 2) the mobilities of the electrolyte co-ion and counter-ion; 3) cell geometry; 4) electrode positioning along the capillary or the microfluidic channel; and 5) operating frequency. The use of a ground plane between the electrodes, electrode tightness, and temperature control should be also addressed to minimize possible sources of noise and consequently increase the sensitivity. A review by Kuban and Hauser [133] described the recent instrumental developments and applications of this detection mode. The analysis of around a hundred papers described in this review shows peak-to-peak voltage varying from 2 to 500 V_{pp} and frequencies between 14 to 625 kHz being used in CE or microchip analysis. Although these parameters were found to be important to determine the absolute value of the C^4D sensitivity, adjustments of these two parameters for different detector implementations seem to lead to similar LODs. Kang *et al.* [134] created a low-impedance C^4D using a piezoelectric quartz crystal (PQC) connected in series with the function generator to reduce the impedance in μchip-CE. The impedance in the detector was reduced because the capacitive reactance from the wall capacitance was compensated by the inductive reactance from the PQC. The operation frequency of the low-impedance C^4D was set at the resonant frequency of the series combination of a PQC with a C^4D, where minimum impedance was obtained at 1MHz for the specific glass microchip. The authors conclude that S/N ratio of the low-impedance C^4D were improved by ~20–50 times over those of a standard C^4D. LODs were 0.38, 0.49, and 1.6 μmol·L^{-1} for K^+ with microchip lid thickness of 0.20, 0.40, and 1.0 mm, respectively. Do Lago's group described in detail a new version of a C^4D electronic circuit considering the following four principles: simplicity, robustness, compactness, and performance [135]. This new version was developed with an integrated 1.1 MHz and 4 V_{pp} sine wave local oscillator and an ADC of 21 bits that eliminates the necessity of baseline compensation by hardware. The circuit works with any noise-free power supply between 7 and 12 V and uses a 20 μm thick copper foil as a ground plane. It was constructed with a lower number of connections to reduce possible sources of noise. The authors also described a clever idea to determine the ID of capillaries from 20 to 100 μm by comparing the signal obtained from capillaries alternately filled with air and water. The LOD for K^+, Ba^+, Ca^{2+}, Na^+, Mg^{2+}, and Li^+ were 0.6, 0.4, 0.3, 0.5, 0.6, and 0.8μmol·L^{-1}, respectively, which is comparable to other high-quality versions of C^4D. Guo *et al.* [136] experimentally examined the impedance of a C^4D detector cell for different parameters (length and cell gap) by alternate current impedance. They concluded that the impedance increases with increasing gap between the electrodes and the length of the electrodes. It was shown that the diameter of the electrode is critical and tightly coupling the electrodes to the outer wall of the capillary is necessary. These results were consistent with the simulations of Brito-Neto [131,132]. New improvements in μchip-CE were also achieved by Coltro *et al.* in 2008. The authors presented a method to fabricate and integrate planar C^4D electrodes on polyester-toner microchips [137]. The electrode material (aluminum) was sputtered over a printed toner mask and remained anchored to the surface after the toner removal (lift-off). The integration of the electrodes to printed channels was provided by a thermal lamination at 120 °C in less than 2 min. These toner-based microdevices can be fabricated in a matter of minutes using low-cost consumables and simple tools. The incorporation of the electrodes in the chip eliminates the problem of manual alignment. The proposed methods also provided more robustness and better reproducibility, emphasizing the great potential of C^4D to be a platform of choice for portable and disposable point-of-care analysis. The LODs (at 400 kHz and 10 V_{pp}) for K^+, Na^+, and Li^+ were,

respectively, 3.1, 4.3, and 7.2 μmol·L^{-1} in less than 90 s under an electric field of 250V/cm. Fercher *et al.* [138] described a novel microchip C^4D device produced in low-temperature co-fired ceramics (LTCC). The application of LTCC multilayer technology allows a broad diversity of electrode arrangements inside and on top of the ceramics and increase the dielectric constant compared with glass or plastics microchips, resulting in better C^4D sensitivity according to the authors. In these experiments, inorganic ions were separated in less than 1 min at 300V/cm with C^4D detection performed at 2.25 MHz, 5 V_{pp}. The LOD of 10μmol·L^{-1} for K^+ was achieved using this ceramic device. The increase in sensitivity argued by the authors has not been confirmed experimentally in literature. LODs of K^+ using polymethyl methacrylate (PMMA), PDMS, or conventional fused silica capillaries are in the same detection range. The lamination process used to build this device consumes around two hours. Wang *et al.* describe a wall-jet conductivity detector for PMMA microchips [139]. The device is based on a "hybrid" arrangement where the receiving electrode is insulated by a thin layer of a dielectric and the emitting electrode is in direct contact with the solution. LODs as low as 3 and 5μmol·L^{-1} (for ammonium and sodium, respectively) were achieved using a sinusoidal frequency of 200 kHz and 10 V_{pp}. The authors suggested that further improvements of the detector sensitivity are expected by application of high-voltage conductivity detection schemes and new detection geometries. Ryvolova *et al.* [42] developed a 3-in-1 detection cell that for the first time allows current single-point detection of three signals: C^4D, photometric and fluorimetric. The single-point preserves the identical times of peaks passing through the detector and the three signals can be easily compared. The gap between the C^4D electrodes of ~7 mm is unusual compared with the traditional ~2 mm. At 50 kHz the LOD of K^+ and Mg^{2+} were 6.4 and 5 μmol·L^{-1}, respectively (around 10 times less sensitive than LOD average to CE or microchip to these cations). Although other conductivity detectors have been recently described [140], it seems like most LODs are stabilized around theμmol·L^{-1} range. This indicates that new electronic developments are necessary to increase the applicability of this powerful yet simple detection technique.

Conductivity detection has been also used in conjuction with a semicontinuous aerosol composition analyzer [141]. The system consisted of a growth tube particle collector coupled to a microfluidic device for chemical analysis. The growth tube enlarges particles through water condensation in a laminar flow, permitting inertial collection into the microchip sample reservoir. For inorganic anions, temporal resolution of 1 min and estimated detection limits of 70 140 ng m ^{3} min were obtained. The system was used to measure sulfate and nitrate, and results were compared to a particle-into-liquid-sampler running in parallel.

Other Detection Modes—Mass spectrometry (MS) has become a well-accepted analytical approach that combines molecular information with separation efficiency. Although a significant number of applications has been described [142–146] and research in areas that go above and beyond simple separation has been recently reviewed [54], the routine use of CE-MS has not kept pace with technical and instrumental developments [146]. When coupling CE and MS, two critical problems must be addressed: 1) grounding the electrical current of the CE separation voltage; and 2) transferring the analytes into the mass spectrometer at maximum efficiency [54,147–150]. To accomplish these, three types of ionization methods (electrospray ionization, or ESI, atmospheric pressure chemical ionization, or APCI, and matrix-assisted laser desorption ionization, or MALDI) and three interface setups (sheathless [151], co-axial sheath flow, and liquid junction) are typically employed. Because it allows the direct transfer of analytes from the liquid phase to the gas phase and the formation of multi-charged ions, ESI has been the preferred ionization method for on-line setups [152–155]. CE–ESI–MS also enables completing the electrical circuit for analyte separation, while simultaneously providing an electrical potential to the spray tip, generally accomplished using sheath-flow interfaces [156]. Recently, the numerical analysis of the mass transport of analytes through the liquid junction interface between the separation and nano-ESI capillaries was described [157]. In the

report, Klepárník and Otevrel identified three operational parameters that can be rationally optimized, if the dynamics of the process are known: 1) the geometry of the interface, especially the width of the gap between the separation and spray capillaries; 2) the electric field strength, controlling the migration of analytes in the separation capillary and in the gap, and 3) the pressure exerted on the gap, controlling the flow rate of the liquid through the spray capillary. A microfabricated fluidic device was developed for the automated real-time analysis of individual cells using CE-ESI-MS [158]. In this case, the chip was mounted on an x-y-z translational stage in front of the atmospheric pressure inlet of a Micromass QTOF Micro mass spectrometer (Waters Corp., Milford, MA). The chip was positioned so the spray corner was approximately 7 mm apart from the mass spectrometer inlet orifice. The feasibility of APCI as an alternative ionization technique for CE-MS was investigated using a grounded sheath-flow CE-MS sprayer and an orthogonal APCI source. The APCI-MS set-up enabled detection of basic, neutral, and acidic compounds, whereas apolar and ionic compounds could not be detected. Background electrolyte composition, sheath-liquid flow rate, and vaporizer temperature can be optimized with respect to the CE separation without affecting the APCI-MS response and reaching detection limits (S/N ratio = 3) in the 2–10 $\mu mol \cdot L^{-1}$ [159]. A PDMS microchip for CE-MALDI-MS has been described by Luo *et al.* [160]. The chip allowed fractionating the separated analytes and pushing the analyte fractions into open reservoirs. Each analyte fraction was then mixed with a matrix solution and deposited on a MALDI target. An overview of chip fabrication, microfluidic components, and the interfacing of these devices to MALDI-MS is also available [161]. Other pertinent reports describing on-line coupling of CE with atmospheric-pressure photoionization [162], a new algorithm to align CE–MS data [150], the performance of various capillary coating strategies used in CE-MS [163], a liquid-junction/low-flow interface [164], and a procedure for collecting fractions during CE for their analysis using various stand-alone instruments [148] have been also described.

Combining the extraordinary separation efficiency of CE with nuclear magnetic resonance (NMR) has yielded unique analytical possibilities. The great strength of NMR spectroscopy is that it can provide, non-destructively and at atomic resolution, molecular information about the samples. For these reasons it is routinely used to identify small molecules, to study structure and reaction dynamics, and to probe a variety of intermolecular interactions [165,166]. Although significant improvements can be made by increasing the observation time, using stronger magnetic fields, or by designing specific detection schemes [167–170], the relatively poor sensitivity of NMR seems to be one of major drawbacks, specially when coupled to CE [171]. Using advances in laser microfabrication techniques, a series of radiofrequency microcoils were developed to produce field deployable, high sensitivity NMR-based detectors [172]. This was followed by the development of a low-cost microcoil CE-NMR system for *in situ* characterization of metal compound speciation [173]. In this case, high-precision laser lithography was used to produce copper sputtered microcoils that have comparable resistivity and quality factors to that of hand wound microcoils. Another strategy to improve the sensitivity of NMR is to couple it with capillary isotachophoresis (cITP). As pointed by Korir and Larive [174], in cITP the sample is injected between plugs of buffer with higher and lower effective electrophoretic mobility, enabling the formation of stable boundaries that remain in contact with each other and travel at constant velocity. In this regard, they constructed a solenoidal microcoil (1 mm long) using 50 μm polyurethane-coated copper wire wrapped around a polyimide sleeve of inner and outer diameters of 370 and 430 μm, respectively (Please insert Figure 4). This setup (Avance Bruker spectrometer, 600 MHz) allowed them to perform on-line NMR detection of microgram quantities of heparin-derived oligosaccharides and to elucidate their structure. A similar instrumental setup was also used to isolate and detect 4-aminophenol in an acetaminophen sample spiked at the 0.1% level, with no interference from the parent compound [175].

Few reports have also described μchip-CE devices with integrated NMR detection [176]. In this regard, a new electromagnetic induction detector with two vertical inductors for CE and μchip-CE was developed [124]. The system consisted of a high-frequency generator (DG1011, Rigol Technologies, Inc.), a high-frequency voltmeter (HFJ-8B, Shanghai Wuyi Electronic Equipment Co., Ltd.), and a simple amplifier made of IC 3140 (Texas Instruments Co., USA). The magnetic core consisted of a cylindrical magnetic conductor (diameter: 2 mm; length: 10 mm) made from non-magnetized ferrate wrapped with enamelled wire (diameter, 0.1 mm). Upon optimizing the detector's response (number of coil turns, frequency, and effective voltage), its feasibility and performance were demonstrated by analyzing inorganic ions (KCl and $MgCl_2$). Although not integrated, several other reports supported the advantages of correlating CE and NMR information [177–179]. As pointed in a recent review [180], due to the optimal premises of both techniques, further developments in CE-NMR are expected to open new research avenues in the near future.

Though used less frequently, other detection methods [181,182] including atomic fluorescence spectrometry [183], inductively coupled plasma MS [147,184,185], atomic absorption spectrometry [186], laser-induced capillary vibration, and surface plasmon resonance [187] are available to monitor CE separations.

2C- Components for CE and μchip-CE

Pumps, valves, actuators and mixers are essential components in many electrophoretic devices. For that reason, a variety of techniques have been used for delivery and control of liquids in CE-sensors and other microfluidic devices. Among others [30,188–191], a description of the principles and some applications of electrophoretic, electro-osmotic, opto-acoustic, optically-driven, electrochemical, and gravity-driven pumps has been recently published [25]. Because they do not require moving parts (motors, actuators, or check valves) and can be controlled with the same instrumentation used to power separation, most pumps used in CE and μchip-CE devices are electro-osmotically-driven. In this regard, a simple bead-packed electro-osmotic pump was designed, fabricated, and theoretically described using models for hydrodynamic and electrokinetic transport in complex porous media [192]. The theoretical analysis yields useful relationships between the parameters of the pump (bead size, capillary size, electrokinetic ζpotential) and its performance (pressure and flow) rate and hence, provides guidelines for optimal design for desired properties. The possibility of using a series of miniature semiconductor diodes embedded in the walls of a microfluidic channel to pump liquid was demonstrated by Chang *et al.* [193]. In this case, the signal to the electrodes was provided by an alternating current generator (FG-7002C, EZ Digital) and amplifier (PZD 700, Trek), and was monitored with an oscilloscope and a digital voltmeter. Yairi and Richter described a voltage-controlled pump based on EOF capable of generating both high flow rates and high pressures [194]. The pump consisted of approximately one half-million microchannels and was able to produce pressures of 5.5 kPa/V and flow rate of 0.054 mL/min/V/cm^2. Xu and co-workers recently described the development and application of a capillary partially coated with poly-vinyl alcohol as an electro-osmotic pump [195]. Similarly, Joo and co-workers [196] used glass coated with either anionic or cationic polymers to produce a rapid (262.4 nL min^{1} when 1.0 kV cm^{1} was applied in 10 $mmol{\cdot}L^{-1}$ phosphate buffer at pH 7.0) field-free electro-osmotic micropump. The different surface charge of the Y-shaped pump produced EOF in opposite directions when an electric field was applied along the two coated arms. The hydrodynamic pressure developed at the common junction of the three arms generated field-free flow, which responded rapidly and reversibly to the applied electric field. Additionally, a simple diaphragm micropump and a single voltage supply were used by Li *et al.* to generate controllable well-defined sample plugs [197]. Ducrée and co-workers described the possibility of using centrifugal forces to integrate liquid handling for sample preparation and subsequent detection [198]. Among other advantages, this approach can operate widely

independent liquid properties (viscosity, electrical conductivity, thermal behavior) and surface tension over a broad range of volumes. Similarly, Kim presented two different methods for a passive flow switching valve on a centrifugal microfluidic platform, which controls the direction of a flowing liquid at a junction where a common inlet and two outlet channels meet [199]. Switching of the flow can be performed either by relying on the Coriolis or by means of the fluidic capacitance of an air pocket trapped between two fluids at a non-symmetric junction. Yoo *et al.* presented a microfluidic system with paraffin-actuated microvalves and a thermopneumatic-actuated micropump that are easily integrated on the microchip substrate using PDMS, indium tin oxide and glass [200]. A maximum pumping rate of about 2.0 μl min^{-1} was measured at a duty ratio of 5% and a frequency of 1 Hz. The flow cut-off powers for the microvalves with the channel depth of 220μm, were 300 and 350 mW for valve seat diameters of 1.5 and 2.0 mm, respectively. Pappas and Holland demonstrated the utility of aqueous phospholipid preparations comprised of 1,2-dimyristoyl-sn-glycero-3-phosphocholine and 1,2-dihexanoyl-sn-glycero-3-phosphocholine for fluid steering in a microfluidic device [201]. Using three copper conduits, a hot/cold circulating water bath, and standard manual valves they were able to achieve a change in flow direction for opening and for closing the channel of 19 ± 1 s (n = 10) and 11 ± 1 s (n = 10), respectively. More recently, Bachman's group reported a bubble-based valve system that is simple in design and fabrication, can be individually addressed electronically, can be easily integrated into existing microfluidic devices without additional manufacturing steps, and requires very little footprint [202]. In the described design, a temperature gradient in the microfluidic channel was used to control the size of an air bubble, which is capable of opening/closing a valve. Leslie and co-workers demonstrated a simple strategy for flow control using fluidic networks with embedded deformable features [203]. These fluidic networks consist of capacitors (a deformable film) and resistors (conventional microchannel) and were operated by modulating the dimensions of the channels and capacitor film and the frequency of a time-modulated pressure source.

Other authors have opted for the use of commercial systems for flow control (pumps and valves) in microfluidic devices. Among others, Fluigent [204–206], Eksigent [207], or LabSmith are some of the many companies offering products that have been used in pertinent publications. It is also worth mentioning that to bond connectors to microfluidic devices, Ng *et al.* investigated the use of ultrasonic welding (Branson 921 AES). Different schemes of the method were explored based on different designs of the connectors to achieve a strong (withstand at least 6 bars), minimal dead-volume connection. Combining the small scale of welding, the use of inserts, and proper fixture designs, they were able to attach PMMA connectors to PMMA chips [208]. Additionally, a novel low dead-volume capillary–capillary interface was fabricated allowing two-dimensional CE separations in a comprehensive mode [209].

3- Compact Systems

This section highlights selected developments of compact CE and μchip-CE systems in academic research, focusing on systems that have all components needed to perform the analysis (HVPS, detection system, *etc.*) in a self-contained format. These systems tend to be highly integrated, portable, and require modest power. Applications include remote analysis for space exploration, hazardous environmental testing, gene sequencing, forensics, and diagnostics.

In 2005, Culbertson *et al.* demonstrated the feasibility of CE separations in reduced-gravity and hypergravity environments [210]. Their portable CE device (Please insert Figure 5) has a glass microchip, two HVPS, a high-voltage switch, a solid-state diode-pumped green laser pointer (The Laser Guy, Houston, TX), and a channel photomultiplier (MD972, Perkin-Elmer Optoelectronics, Santa Clara, CA) for detection, among other optical components. An inertial mass measurement unit (ADXL105EM-3, Analog Devices, Norwood, MA) was included to

measure the gravitational environment during analysis. The entire device, enclosed in a 28 x 38.4 x 16 cm acrylonitrile butadiene styrene and polycarbonate box, can be powered by 10 D-cell alkaline batteries. The device successfully demonstrated the separation and detection of labeled amino acids under low gravity conditions, though some drift was observed.

One of the most highly developed and integrated CE systems designed for space exploration is the Mars Organic Analyzer (MOA). This system was developed in 2005 by Richard Mathies' group [211] as an alternative to the former gas chromatography-MS method of detection of biomarkers of life on Mars [212,213]. The MOA includes a microfabricated chip with membrane valves and pumps, a sipper for sampling, and a CE separation channel. Three miniature HVPS and one high-voltage solid-state switch are used to produce and control the potential for electrophoresis and to float the anode. Two rotary pumps actuate pneumatic components for the pumps and valves, and a thermoelectric cooler maintains the temperature of the separation channel at 8°C. Detection is accomplished by LIF with a 400 nm diode laser (CrystaLaser, Reno, NV), 430 nm dichroic beam splitter, objective lens, 430 nm long-pass and 522 nm band-pass filters, and a 100 μm-diameter fiber-optic-coupled photomultiplier [211]. The MOA was initially used to analyze fluorescamine-derivitized amino acids and their chirality [211]. Further work has extended its use to the analysis of nucleobases and other amine-containing biomarker compounds [214], neuroactive bioamines in food products [215], and polycyclic aromatic hydrocarbons [216]. Re-optimization of conditions has allowed the analysis of samples in highly acidic or saline conditions [217] and the use of Pacific Blue as a derivatizing agent has significantly lowered detection limits of the MOA. Recently, Benhabib *et al*. have improved the instrumentation as well as the microchip in the latest version of the CE system-the Multichannel Mars Organic Analyzer, or McMOA [218]. The instrument is now autonomous, has integrated sample preparation (sample retrieval, sample distribution, and cleaning) and has been expanded to eight independent separation channels. The optical components for LIF detection include a compact 405 nm diode laser (FiberTEC405, Blue Sky Research, Milpitas, CA), linear scanning objective, and CCD array detector spectrometer (USB4000, Ocean Optics, FL). Portable CE instruments have also been developed for use in hazardous environments. In 2009, Seiman *et al*. demonstrated the use of a battery-powered CE device for detection of the degradation products of chemical warfare agents in soil extracts [219]. The portable device, with dimensions of 330 x 180 x 130 mm, simply contains a cross-sampler for injection into the separation capillary (EMCO DX250 HVPS, Sutter Creek, CA) and employs a lab-built C^4D detection system.

In 2006, Easley *et al*. reported the design of a microfluidic genetic analysis system capable of accepting crude biological samples (e.g. whole blood) and generating a genetic profile [220]. The chip has two sample preparation domains: nucleic acid purification through solid-phase extraction, and target sequence amplification by polymerase chain reaction (PCR). Fluid is driven by a syringe pump and valves direct the flow. The amplicons then pass through an electrophoresis-LIF analytical domain. The custom-built dual-polarity HVPS is comprised of two Spellman high-voltage sources (Hauppauge, NY). LIF detection is achieved by excitation through an Argon ion laser (Model LS200, Dynamic Laser, Salt Lake City, UT) and emission is collected by a PMT and a 515 nm bandpass filter in a conventional confocal detection setup [220]. The article suggests that the system can be assembled into a portable system for use in clinical, forensic, and biowarfare defense applications. Kaigala *et al*. demonstrated cost-effective fabrication of a portable and integrated microchip-based reverse transcriptase-PCR-CE system for genetic analysis in 2008 [221]. The system includes a glass-PDMS microchip with integrated pneumatic valves and pumps for fluid control and a resistive thin-film heater and temperature sensor element. The optical detection components include a laser diode and a CCD camera. All components for the system totaled about $1,000 [221]. In 2006, the Mathies group reported a system capable of nanoliter-scale Sanger DNA sequencing [222]. The microchip has regions for the three major steps of the process: thermal cycling, controlled by

a surface heater (7.8 Ω, Minco, Minneapolis) and resistive temperature detector, sample purification, and CE with LIF detection by the Berkeley confocal rotary scanner [223]. Since this system can be used to perform fundamental operations such as DNA amplification, nucleic acid concentration/purification, and DNA-fragment size determination, it is useful in a wide range of applications. The Mathies' group then took a first step toward a multichannel PCR-CE system capable of four parallel analyses [224]. They used a similar device to perform reverse transcription-PCR for gene expression and biomarker analysis [225]. Next, the group reported the design of a portable PCR-CE microdevice for short tandem repeat analysis. The fully integrated system, which can be powered with 20 W, has redesigned electronics for uniform temperature during PCR, pneumatics for microfluidic manipulation, four HVPS for CE, a 488 nm frequency-doubled diode laser (Protera, Novalux Corp., Sunnyvale, CA) and an optical system for four-color fluorescence detection [226].

Some drawbacks of including PMTs in detection systems include high cost and bulky size, especially in sequencing applications when detection of four bases requires four PMTs. Rech *et al*. validated the use of solid-state single photon avalanche diode (SPAD) array detectors for DNA fragments in 2006 [227]. SPAD sensors have high sensitivity and allow significant miniaturization of genetic analysis systems along with simplicity, low power consumption, and reduced cost compared to PMTs or CCDs. Recently, the group produced an ultra-compact complete genetic analysis system comprised of custom and low-cost components. The separation microchip (Micronit) is only 45 x 15 x 1.8 mm with separation channels that are 50 μm wide. Injection and separation potentials are produced and controlled by three independent HVPS developed from an ultra-compact high-voltage DC converter (EMCO). After electrophoretic separation, the fluorescent markers on the DNA fragments are excited with two low-cost and compact laser diodes (TOLD 9442 by Toshiba and L7910 by Hamamatsu) instead of bulky Argon lasers. The emissions pass through optical filters (Chroma Technology USA) and are collected by a microscope objective. The four remaining wavelengths separate by a transmission grating (6001/mm Thorlabs) and then are focalized on a monolithic array of 4 SPAD detectors (IMM-CNR, Bologna). The size of the entire module is merely 19 x 12.5 x 15 cm [228].

In 2008, the first prototype of a *lab-on-a-robot* device was presented by Berg *et al.* [229]. The system is capable of collecting a gas sample, performing the subsequent analysis (injection, separation, and detection), and sending the data to a distant control unit. The operation of the *lab-on-a-robot* (Please insert Figure 6A) begins by selecting the strategic geographic location of the mobile unit employing global positioning systems (GPS) and transmitted video. Subsequently, using a LabVIEW graphical user interface (GUI) for communication, the robot's peripherals are transferred from mobility to chemical detection and the testing specifications are transmitted from a base station and stored in the robot. Next, a micro-actuated pump (model mp5, Bartels Mikrotechnik, Dortmund, Germany) is activated to diffuse a gaseous sample through a 150 μm ID fused silica capillary and into the sample reservoir on the chip. Next, an aliquot of the sample is injected (pinched injection) and the components are electrophoretically separated. While the test is running, detection current as a function of time is transmitted to a personal computer and a real time electropherogram can be produced through the GUI. As shown in Please insert Figure 6B, the capabilities of the systems were demonstrated by analyzing a sample of air containing phenol and using ferulic acid as the internal standard.

Although most attempts at miniaturizing CE systems have focused on the use of microfluidic devices as separation platforms, it has been demonstrated that systems can be designed to be portable while still using capillary tubing for electrophoretic separations. In 2007, Kuban *et al*. designed and field-tested a portable, battery-powered CE system with integrated contactless conductivity detection for detection of ionic compounds in environmental samples [40]. Though the separation is conducted in a silica capillary (as opposed to a microchip channel),

the unit is still a compact 70 mm x 205 mm x 160 mm. Other non-chip based portable CE systems have been reviewed recently [230].

4- Innovative Uses and Modifications of Classic CE Instrumentation

The most basic instrumental setup for a CE includes a couple of vials containing either background electrolyte or sample, a capillary tube (50–150 μm ID), a power supply, and a detector. Most commercial instruments also contain a pressure/vacuum system to perform hydrodynamic injections and to rinse the capillary between runs. Although this setup has proven to be extremely effective to perform separations, other uses have been also reported. The objective of including this section is to highlight a few examples of conventional instruments that function beyond the quantification of a group of analytes to expand the capabilities of current laboratories, and to enable new training opportunities for students.

Since 1995, several reports have described the use of CE instrumentation for the determination of critical micellar concentration (CMC) values [231–234]. Recently, Stanley *et al.* reported a fast (~4 min) method for the determination of CMC values that uses CE instrumentation to monitor relative viscosity changes [235]. Similarly, a CE instrument was used to measure viscosity, conductivity and absorbance of pure ionic liquids and ionic liquid–molecular solvent mixtures using minimum sample volumes (~50 μL) [236]. In order to characterize both protein-ligand binding as well as protein hydrodynamic radius, Taylor dispersion analysis and CE were combined. Using two different systems (glycosylated human serum proteins and albumin interacting with propranolol) and frontal analysis mode, binding constants and hydrodynamic radii were obtained and correlated by independent methods [237]. Similarly, the effect of separation parameters such as ligand concentration and CE voltage on the separation dynamics of α-fetoproteins was investigated. Bharadwaj *et al.* described a comprehensive mathematical model to predict electropherograms for affinity-based (nonequilibrium conditions) separations [238]. The model includes the effects of molecular diffusion, electromigration, nonequilibrium reaction, and detection process. Other examples of frontal analysis have been also reported [239]. The collective diffusion coefficient (D_C) of diluted suspensions of positively-charged iron oxide maghemite nanoparticles was also investigated using a CE instrument on the grounds of Taylor dispersion theory [240]. CE has been also used to determine the size of water-soluble CdSe/ZnS core-shell quantum dots [241] and the electrophoretic mobility of colloidal particles [242]. Mora *et al.* used a CE to investigate the adsorption of surfactants to PDMS-coated capillaries and to develop a simple model to estimate the EOF as a function of the structure of the surfactant and its concentration [38].

The use of a modified instrument (Beckman P/ACE MDQ) with on-column LIF detection for the automated analysis of individual latex particles in solution was also reported [243]. The modification included an external input/output (I/O) board that allowed for faster data acquisition rates (e.g. 100 Hz) than those available with the standard instrument settings (e.g. 4 Hz). This system opened exciting possibilities for those interested in the study and analyses of organelles, liposomes, and nanoparticles [244].

Reijenga and co-workers showed that different operating temperatures (a custom-programmed CE) can be used to fine-tune the separation. The same group also proposed specific ways of programming the instrument (Beckmann P/ACE 5500) and performing a sequential electrokinetic injection [245]. Using an EOF marker as a sample to find optimal conditions for cross-correlation experiments, S/N ratio improvements of around 2.8 (compared to 4.0 theoretical) were obtained. Although not available in most basic instruments, a LIF photobleaching anemometer was developed for measuring fluid flow velocity in a microfluidic instrument in less than 10 min at extremely low cost [246].

The use of two additional reservoirs to accommodate the electrodes of the power source was proposed to improve the stability of the running electrolyte in CE [247]. The basic idea is to use salt bridges to connect those reservoirs to the ones containing the capillary ends. According to the report, the electrolysis-separated system enabled performing at least 15 runs without observing significant changes in the migration time or resolution, allowing the preparation of running electrolytes with electroactive species or using unbuffered solutions. The same group also presented a clever and simple way to monitor the EOF in CE using thermal marks [248]. The so-called thermal mark is a perturbation of the electrolyte concentration generated by a punctual heating of the capillary (provided by a tungsten filament or a resistor, see Please insert Figure 7) while the separation electric field is maintained. The thermal mark was recorded with a conductivity detector (described elsewhere [41,135]) as part of a usual electropherogram and used to index the analyte peaks and thus compensate for variations of the EOF. This is an excellent example of how few resources could be used to develop useful instrumentation.

5- Conclusions

This review intended to provide a broad view of recent instrumentation dedicated to improve the performance of CE and μchip-CE devices. A quick bibliography search shows that the development of optical detectors (in particular, LED-based systems) and components (valves, pumps, *etc*.) are some of the most active fields in the last five years. On the contrary, few developments in HVPS have been recently published. Outstanding achievements have been found in regards to the developments of compact systems and detection devices, enabling the analysis of a wide variety of samples and, in the case of MS and NMR, obtaining structural information of the components of a mixture. It is therefore expected that future developments in instrumentation will enable closing the gap between the current technologies and true lab-on-a-chip devices for general analytical needs.

List of Abbreviations

μchip-CE	microchip-capillary electrophoresis
ADC	analog-to-digital converter
APCI	atmospheric pressure chemical ionization
C^4D	capacitively-coupled contactless conductivity detection
DC	direct current
ECD	electrochemical detection
ESI	electrospray ionization
GPS	global positioning system
GUI	graphical user interface
HVPS	high-voltage power supply
ID	inner diameter
LCORR	liquid core optical ring resonator
LTCC	low-temperature co-fired ceramics
McMOA	Multichannel Mars Organic Analyzer
MOA	Mars Organic Analyzer
PEPS	programmable eight-path-electrode power supply
PMT	photomultiplier tube

PQC	piezoelectric quartz crystal
RI	refractive index
RIU	refractive index units
SPAD	single photon avalanche diode
USB	universal serial bus
WGM	whispering gallery mode

6- References

1. Kim P, Albarella JD, Carey JR, Placek MJ, Sen A, Wittrig AE, McNamara WB Iii. Sens Actuators, B 2008;134:307–312.
2. Camou S, Shimizu A, Horiuchi T, Haga T. Sens Actuators, B 2008;132:601–607.
3. Nakajima H, Harada Y, Asano Y, Nakagama T, Uchiyama K, Imato T, Soh N, Hemmi A. Talanta 2006;70:419–425. [PubMed: 18970786]
4. Shankaran DR, Gobi KV, Miura N. Sens Actuators, B 2007;121:158–177.
5. Elmi I, Zampolli S, Cozzani E, Mancarella F, Cardinali GC. Sens Actuators, B 2008;135:342–351.
6. Baschirotto A, Capone S, D'Amico A, Di Natale C, Ferragina V, Ferri G, Francioso L, Grassi M, Guerrini N, Malcovati P, Martinelli E, Siciliano P. Sens Actuators, B 2008;130:164–174.
7. Rivera L, Puyol M, Villuendas F, Alonso J. Sens Actuators, B 2008;134:863–868.
8. Yang M, Kim T-Y, Hwang H-C, Yi S-K, Kim D-H. J Am Soc Mass Spectrom 2008;19:1442–1448. [PubMed: 18565759]
9. Nimal AT, Mittal U, Singh M, Khaneja M, Kannan GK, Kapoor JC, Dubey V, Gutch PK, Lal G, Vyas KD, Gupta DC. Sens Actuators, B 2009;135:399–410.
10. Zampolli S, Elmi I, Mancarella F, Betti P, Dalcanale E, Cardinali GC, Severi M. Sens Actuators, B 2009;141:322–328.
11. Zhong Q, Steinecker WH, Zellers ET. Analyst 2009;134:283–293. [PubMed: 19173051]
12. Benvenuto A, Guarnieri V, Lorenzelli L, Collini C, Decarli M, Adami A, Potrich C, Lunelli L, Canteri R, Pederzolli C. Sens Actuators, B 2008;130:181–186.
13. Yang Y, Chae J. J Micromech Microeng 2008;18:125010.
14. Liu J, Chen C-F, Tsao C-W, Chang C-C, Chu C-C, DeVoe DL. Anal Chem 2009;81:2545–2554. [PubMed: 19267447]
15. Collins GE, Lu Q. Anal Chim Acta 2001;436:181–189.
16. Kaigala GV, Hoang VN, Stickel A, Lauzon J, Manage D, Pilarski LM, Backhouse CJ. Analyst 2008;133:331–338. [PubMed: 18299747]
17. Gauthier GL, Grimm R. Drug Discovery Today: Technologies 2006;3:59–66.
18. Wu D, Qin J, Lin B. J Chromatogr A 2008;1184:542–559. [PubMed: 18207148]
19. García-Pérez I, Vallejo M, García A, Legido-Quigley C, Barbas C. J Chromatogr A 2008;1204:130–139. [PubMed: 18656201]
20. Rassi ZE. Electrophoresis 2009;31:174–191. [PubMed: 20039288]
21. Verpoorte E. Electrophoresis 2002;23:677–712. [PubMed: 11891702]
22. Sinville R, Soper SA. J Sep Sci 2007;30:1714–1728. [PubMed: 17623451]
23. Chen G, Lin Y, Wang J. Talanta 2006;68:497–503. [PubMed: 18970349]
24. Kraly JR, Holcomb RE, Guan Q, Henry CS. Anal Chim Acta 2009;653:23–35. [PubMed: 19800473]
25. Chen L, Lee S, Choo J, Lee EK. J Micromech Microeng 2008;18:013001.
26. Oh KW, Ahn CH. J Micromech Microeng 2006;16:R13.
27. Nguyen NT, Wu Z. J Micromech Microeng 2005;15:R1.
28. Kuswandi B, Nuriman Huskens J, Verboom W. Anal Chim Acta 2007;601:141–155. [PubMed: 17920386]

29. Swinney K, Bornhop DJ. Electrophoresis 2000;21:1239–1250. [PubMed: 10826668]
30. Dittrich PS, Tachikawa K, Manz A. Anal Chem 2006;78:3887–3908. [PubMed: 16771530]
31. Geschke, O.; Klank, H.; Telleman, P., editors. Microsystem Engineering of Lab-on-a-Chip Devices. Wiley-VCH Verlag GmbH & Co. KGaA; 2008.
32. Ryvolová M, Macka M, Preisler J. TrAC Trends in Anal Chem 2010;29:339–353.
33. Roman GT, Kennedy RT. J Chromatogr A 2007;1168:170–188. [PubMed: 17659293]
34. Rathore, AS.; Guttman, A., editors. Electrokinetic Phenomena. Marcel Dekker; New York, NY: 2003.
35. da Silva JAF, do Lago CL. Anal Chem 1998;70:4339–4343.
36. Preisler J, Yeung ES. Anal Chem 1996;68:2885–2889.
37. Tanyanyiwa J, Hauser PC. Electrophoresis 2004;25:3010–3016. [PubMed: 15349942]
38. Mora MF, Giacomelli CE, Garcia CD. Anal Chem 2007;79:6675–6681. [PubMed: 17676757]
39. Saito RM, Brito-Neto JGA, Lopes FS, Blanes L, Costa ETd, Vidal DTR, Hotta GM, Lago CLd. Anal Methods 2010;2:164–170.
40. Kubán P, Nguyen Huong Thi A, Macka M, Haddad Paul R, Hauser Peter C. Electroanal 2007;19:2059–2065.
41. da Silva JAF, Guzman N, do Lago CL. J Chromatogr A 2002;942:249–258. [PubMed: 11826873]
42. Ryvolova M, Preisler J, Foret F, Hauser PC, Krasensky P, Paull B, Macka M. Anal Chem 2009;82:129–135. [PubMed: 19961219]
43. Hartman DR, Courtney WH. J Chem Ed 1990;67:703.
44. Dasgupta PK, Liu S. Anal Chem 1994;66:3060–3065.
45. Kappes T, Galliker B, Schwarz MA, Hauser PC. TrAC Trends Anal Chem 2001;20:133–139.
46. Zerbinati O. Anal Chim Acta 2003;93:325–327.
47. Jackson DJ, Naber JF, Roussel TJ Jr, Crain MM, Walsh KM, Keynton RS, Baldwin RP. Anal Chem 2003;75:3311–3317.
48. Garcia CD, Liu Y, Anderson P, Henry CS. Lab Chip 2003;3:331–335.
49. Erickson D, Sinton D, Li D. Lab Chip 2004;4:87–90. [PubMed: 15052345]
50. Collins GE, Wu P, Lu Q, Ramsey JD, Bromund RH. Lab Chip 2004;4:408–411. [PubMed: 15269813]
51. Jiang L, Jiang X, Lu Y, Dai Z, Xie M, Qin J, Lin B. Electrophoresis 2007;28:1259–1264. [PubMed: 17377944]
52. Li Q, Zhang H, Wang Y, Tang B, Liu X, Gong X. Sens Actuators, B 2009;136:265–274.
53. Mogensen KB, Klank H, Kutter JP. Electrophoresis 2004;25:3498–3512. [PubMed: 15565705]
54. Nesbitt CA, Zhang H, Yeung KKC. Anal Chim Acta 2008;627:3–24. [PubMed: 18790124]
55. Li X, Tong Y-L, Liu C, Li O-L, Yang X-J, Chen Z-G. Chin J Anal Chem 2009;37:1547–1554.
56. Pan T, Kelly RT, Asplund MC, Woolley AT. J Chromatogr A 2004;1027:231–235. [PubMed: 14971507]
57. Felhofer, JL.; Garcia, CD.; Hanrahan, G.; Gomez, FA., editors. Chemometric Methods in Capillary Electrophoresis. Wiley; New York, NY: 2009.
58. Miyado T, Wakida S-i, Aizawa H, Shibutani Y, Kanie T, Katayama M, Nose K, Shimouchi A. J Chromatogr A 2008;1206:41–44. [PubMed: 18692851]
59. Steiner SA, Fritz JS. J Chromatogr A 2008;1192:152–156. [PubMed: 18405906]
60. Fouad M, Jabasini M, Kaji N, Terasaka K, Tokeshi M, Mizukami H, Baba Y. Electrophoresis 2008;29:2280–2287. [PubMed: 18446802]
61. Lacher NA, Wang Q, Roberts RK, Holovics HJ, Aykent S, Schlittler MR, Thompson MR, Demarest CW. Electrophoresis 2010;31:448–458. [PubMed: 20119952]
62. Caruso CS, de Fátima Travensolo R, de Campus Bicudo R, de Macedo Lemos EG, Ulian de Araújo AP, Carrilho E. Microb Pathogenesis 2009;47:118–127.
63. Giannini I, Orlandini S, Gotti R, Pinzauti S, Furlanetto S. Talanta 2009;80:781–788. [PubMed: 19836552]
64. Cao X-D, Fang Q, Fang Z-L. Anal Chim Acta 2004;513:473–479.
65. Collins GE, Lu Q, Pereira N, Wu P. Talanta 2007;72:301–304. [PubMed: 19071618]
66. Gao Q, Araia M, Leck C, Emmer Å. Anal Chim Acta 2010;662:193–199. [PubMed: 20171319]

67. Whitmore CD, Essaka D, Dovichi NJ. Talanta 2009;80:744–748. [PubMed: 19836546]
68. Rodat A, Kalck F, Poinsot V, Feurer B, Couderc F. Electrophoresis 2008;29:740–746. [PubMed: 18200637]
69. Belin GK, Gärtner V, Seeger S. J Chromatogr B 2009;877:3753–3756.
70. Ziolkowska K, Jedrych E, Kwapiszewski R, Lopacinska J, Skolimowski M, Chudy M. Sens Actuators, B 2010;145:533–542.
71. Chen S, Liu B-F, Fu L, Xiong T, Liu T, Zhang Z, Huang Z-L, Lu Q, Zhao Y-D, Luo Q. J Chromatogr A 2006;1109:160–166. [PubMed: 16325835]
72. Xu B, Yang M, Wang H, Zhang H, Jin Q, Zhao J, Wang H. Sens Actuators, A 2009;152:168–175.
73. Veledo MT, Pelaez-Lorenzo C, Gonzalez R, de Frutos M, Diez-Masa JC. Anal Chim Acta 2010;658:81–86. [PubMed: 20082778]
74. Yu C-Z, He Y-Z, Xie H-Y, Gao Y, Gan W-E, Li J. J Chromatogr A 2009;1216:4504–4509. [PubMed: 19329123]
75. Morgan NY, Wellner E, Talbot T, Smith PD, Phillips TM. J Chromatogr A 2006;1105:213–219. [PubMed: 16359684]
76. Lin S-W, Chang G-L, Lin C-H. J Chromatogr A 2008;1192:198–201. [PubMed: 18407282]
77. Lin S-W, Hsu J-H, Chang C-H, Lin C-H. Biosens Bioelectron 2009;25:450–455. [PubMed: 19720517]
78. Schulze P, Ludwig M, Belder D. Electrophoresis 2008;29:4894–4899. [PubMed: 19025868]
79. Götz S, Karst U. Sens Actuators, B 2007;123:622–627.
80. Yang B, Tan F, Guan Y. Talanta 2005;65:1303–1306. [PubMed: 18969945]
81. Yang B, Tian H, Xu J, Guan Y. Talanta 2006;69:996–1000. [PubMed: 18970670]
82. Arráez-Román D, Fernández-Sánchez JF, Cortacero-Ramírez S, Segura-Carretero A, Fernández-Gutiérrez A. Electrophoresis 2006;27:1776–1783. [PubMed: 16645941]
83. Xu J, Xiong Y, Chen S, Guan Y. Talanta 2008;76:369–372. [PubMed: 18585292]
84. Heras GAB, Breadmore MC, Johns C, Hutchinson JP, Hilder EF, López-Mahía P, Haddad PR. Electrophoresis 2008;29:3032–3037. [PubMed: 18655039]
85. Segura-Carretero A, Fernández-Sánchez JF, Fernández-Gutiérrez A. Biosens Bioelectron 2009:221–237.
86. Yang F-B, Pan J-Z, Zhang T, Fang Q. Talanta 2009;78:1155–1158. [PubMed: 19269486]
87. Krmová L, Stjernlof A, Mehlen S, Hauser PC, Abele S, Paull B, Macka M. Analyst 2009;134:2394–2396. [PubMed: 19918606]
88. Zhu H, White IM, Suter JD, Zourob M, Fan X. Anal Chem 2007;79:930–937. [PubMed: 17263318]
89. Merfort C, Seibel K, Watty K, Böhm M. Microelectron Eng 2010;87:712–714.
90. Guo L, Qiu B, Jiang Y, You Z, Lin J-M, Chen G. Electrophoresis 2008;29:2348–2355. [PubMed: 18435494]
91. Gao Y, Xu Y, Han B, Li J, Xiang Q. Talanta 2009;80:448–453. [PubMed: 19836502]
92. Tryka S. J Quant Spectrosc Radiat Transfer 2009;110:1864–1878.
93. Mandaji M, Buckup T, Rech R, Correia RRB, Kist TL. Talanta 2007;71:1998–2002. [PubMed: 19071554]
94. Martin RS, Gawron AJ, Lunte SM, Henry CS. Anal Chem 2000;72:3196–3202. [PubMed: 10939387]
95. Garcia CD, Henry CS. Electroanalysis 2005;17:1125–1131.
96. Xu J-J, Wang A-J, Chen H-Y. TrAC Trends in Anal Chem 2007;26:125–132.
97. Wang J. Electroanalysis 2005;17:1133–1140.
98. Barry RC, Lin Y, Wang J, Liu G, Timchalk CA. J Expos Sci Environ Epidemiol 2008;19:1–18.
99. Xu X, Zhang S, Chen H, Kong J. Talanta 2009;80:8–18. [PubMed: 19782186]
100. Smith J, Hinson-Smith V. Anal Chem 2002;74:539 A–541 A. [PubMed: 11838672]
101. Trojanowicz M. Anal Chim Acta 2009;653:36–58. [PubMed: 19800474]
102. Pozo-Ayuso DF, Castaño-Álvarez M, Fernández-la-Villa A, García-Granda M, Fernández-Abedul MT, Costa-García A, Rodríguez-García J. J Chromatogr A 2008;1180:193–202. [PubMed: 18177663]

103. Quaiserová-Mocko V, Novotný M, Schaefer LS, Fink GD, Swain GM. Electrophoresis 2008;29:441–447. [PubMed: 18081202]
104. Chen IJ, Lindner E. Anal Chem 2009;81:9955–9960. [PubMed: 19925010]
105. Kong D, Chi Y, Chen L, Dong Y, Zhang L, Chen G. Electrophoresis 2009;30:3489–3495. [PubMed: 19728303]
106. Holcomb RE, Kraly JR, Henry CS. Analyst 2009;134:486–492. [PubMed: 19238284]
107. Chicharro M, Sánchez A, Zapardiel A, Rubianes MD, Rivas G. Anal Chim Acta 2004;523:185–191.
108. Dossi N, Toniolo R, Pizzariello A, Susmel S, Perennes F, Bontempelli G. J Electroanal Chem 2007;601:1–7.
109. Fischer DJ, Hulvey MK, Regel AR, Lunte SM. Electrophoresis 2009;30:3324–3333. [PubMed: 19802847]
110. Ríos A, Escarpa A, González MC, Crevillén AG. TrAC Trends in Anal Chem 2006;25:467–479.
111. Ding Y, Ayon A, Garcia CD. Anal Chim Acta 2007;584:244–251. [PubMed: 17386611]
112. Garcia CD, Henry CS. Anal Chem 2003;75:4778–4783. [PubMed: 14674454]
113. Martin RS, Ratzlaff KL, Huynh BH, Lunte SM. Anal Chem 2002;74:1136–1143. [PubMed: 11924975]
114. Vickers JA, Henry CS. Electrophoresis 2005;26:4641–4647. [PubMed: 16294295]
115. Lin K-W, Huang Y-K, Su H-L, Hsieh Y-Z. Anal Chim Acta 2008;619:115–121. [PubMed: 18539183]
116. Mecker LC, Martin RS. Anal Chem 2008;80:9257–9264. [PubMed: 19551945]
117. Bowen AL, Martin RS. Electrophoresis 2009;30:3347–3354. [PubMed: 19739137]
118. Ertl P, Emrich CA, Singhal P, Mathies RA. Anal Chem 2004;76:3749–3755. [PubMed: 15228350]
119. Inoue J, Kaneta T, Imasaka T. J Capill Electrophor Microchip Technol 2007;10:69–73. [PubMed: 18232516]
120. Castano-Alvarez M, Fernandez-Abedul MT, Costa-Garcia A. J Chromatogr A 2006;1109:291–299. [PubMed: 16472530]
121. Zhang Z, Zhang M, Zhang S. Electrophoresis 2009;30:3449–3457. [PubMed: 19728307]
122. Joo G-S, Jha SK, Kim Y-S. Curr Appl Phys 2009;9:e222–e224.
123. Paul V, et al. J Micromech Microeng 2009;19:077001.
124. Chen, Z-g; Li, O-l; Liu, C.; Yang, X-j. Sens Actuators, B 2009;141:130–133.
125. Desmond D, Lane B, Alderman J, Hill M, Arrigan DWM, Glennon JD. Sens Actuators, B 1998;48:409–414.
126. Chan F-L, et al. J Micromech Microeng 2008;18:075028.
127. Chandra S, Ismail ABM. Sens Actuators, A 2009;154:65–68.
128. Gas B, Demjaneko M, Vacik J. J Chromatogr 1980;192:253–257.
129. Zemann AJ, Schnell E, Volgger D, Bonn GK. Anal Chem 1998;70:563–567.
130. Pumera M. Talanta 2007;74:358–364. [PubMed: 18371649]
131. Brito-Neto José Geraldo A, Fracassi da Silva José A, Blanes L, do Lago Claudimir L. Electroanal 2005;17:1198–1206.
132. Brito-Neto José Geraldo A, Fracassi da Silva José A, Blanes L, do Lago Claudimir L. Electroanal 2005;17:1207–1214.
133. Kubán P, Hauser PC. Anal Chim Acta 2008;607:15–29. [PubMed: 18155405]
134. Kang Q, Shen D, Li Q, Hu Q, Dong J, Du J, Tang B. Anal Chem 2008;80:7826–7832. [PubMed: 18781773]
135. Mendonça KJ, do Lago CL. Electrophoresis 2009;30:3458–3464. [PubMed: 19757437]
136. Guo CC, Guang LL, Jun SY, Ping LY. Electrochim Acta 2009;54:6959–6962.
137. Coltro WKT, Silva JAFd, Carrilho E. Electrophoresis 2008;29:2260–2265. [PubMed: 18446805]
138. Fercher G, Smetana W, Vellekoop MJ. Electrophoresis 2009;30:2516–2522. [PubMed: 19588458]
139. Wang J, Chen G, Muck A. Talanta 2009;78:207–211. [PubMed: 19174226]
140. Míka J, Opekar F, Coufal P, Stulík K. Anal Chim Acta 2009;650:189–194. [PubMed: 19720191]

141. Noblitt SD, Lewis GS, Liu Y, Hering SV, Collett JL, Henry CS. Anal Chem 2009;81:10029–10037. [PubMed: 19904999]
142. Klampfl CW. Electrophoresis 2006;27:3–34. [PubMed: 16315165]
143. Smyth WF. Electrophoresis 2006;27:2051–2062. [PubMed: 16637016]
144. Scriba GKE. J Chromatogr A 2007;1159:28–41. [PubMed: 17316665]
145. Li J, Richards JC. Mass Spectrom Rev 2007;26:35–50. [PubMed: 16967446]
146. Timerbaev AR. TrAC Trends in Anal Chem 2009;28:416–425.
147. Sonke JE, Salters VJM. J Chromatogr A 2007;1159:63–74. [PubMed: 17543311]
148. Helmja K, Borissova M, Knjazeva T, Jaanus M, Muinasmaa U, Kaljurand M, Vaher M. J Chromatogr A 2009;1216:3666–3673. [PubMed: 19147148]
149. Varenne A, Descroix S. Anal Chim Acta 2008;628:9.
150. Nevedomskaya E, Derks R, Deelder A, Mayboroda O, Palmblad M. Anal Bioanal Chem 2009;395:2527–2533. [PubMed: 19826795]
151. Zamfir AD. J Chromatogr A 2007;1159:2–13. [PubMed: 17428492]
152. Nel AL, Krenkova J, Kleparnik K, Smadja C, Taverna M, Viovy J-L, Foret F. Electrophoresis 2008;29:4944–4947. [PubMed: 19025861]
153. Maxwell EJ, Chen DDY. Anal Chim Acta 2008;627:25–33. [PubMed: 18790125]
154. Oh E, Hasan MN, Jamshed M, Park SH, Hong H-M, Song EJ, Yoo YS. Electrophoresis 2009;31:74–92. [PubMed: 20039294]
155. Maxwell EJ, Zhong X, Zhang H, Zeijl Nv, Chen DDY. Electrophoresis 2010;31:1130–1137. [PubMed: 20196027]
156. Monton MRN, Soga T. J Chromatogr A 2007;1168:237–246. [PubMed: 17376458]
157. Klepárník K, Otevrel M. Electrophoresis 2010;31:879–885. [PubMed: 20191549]
158. Mellors JS, Jorabchi K, Smith LM, Ramsey JM. Anal Chem 2010;82:967–973. [PubMed: 20058879]
159. Hommerson P, Khan AM, de Jong GJ, Somsen GW. J Am Soc Mass Spectrom 2009;20:1311–1318. [PubMed: 19349196]
160. Luo Y, Xu S, Schilling JW, Lau KH, Whitin JC, Yu TTS, Cohen HJ. JALA 2009;14:252–261.
161. Lee J, Soper SA, Murray KK. Anal Chim Acta 2009;649:180–190. [PubMed: 19699392]
162. Mol R, Jong GJd, Somsen GW. Electrophoresis 2005;26:146–154. [PubMed: 15624178]
163. Huhn C, Ramautar R, Wuhrer M, Somsen G. Anal Bioanal Chem 2010;396:297–314. [PubMed: 19838682]
164. Hsueh Y-H, Huang J-L, Tseng M-C, Her G-R. Electrophoresis 2010;31:1138–1143. [PubMed: 20209568]
165. Wensink H, Benito-Lopez F, Hermes DC, Verboom W, Gardeniers HJGE, Reinhoudt DN, Berg Avd. Lab Chip 2005;5:280–284. [PubMed: 15726204]
166. Edison AS, Long JR. Nature 2007;447:646–647. [PubMed: 17554293]
167. Wolters AM, Jayawickrama DA, Sweedler JV. Curr Opin Chem Biol 2002;6:711–716. [PubMed: 12413558]
168. Li Y, Logan TM, Edison AS, Webb A. J Magn Reson 2003;164:128–135. [PubMed: 12932464]
169. McDonnell EE, Han S, Hilty C, Pierce KL, Pines A. Anal Chem 2005;77:8109–8114. [PubMed: 16351162]
170. Lee H, Sun E, Ham D, Weissleder R. Nat Med 2008;14:869–874. [PubMed: 18607350]
171. Jayawickrama DA, Sweedler JV. J Chromatogr A 2003;1000:819–840. [PubMed: 12877202]
172. Demas V, Herberg JL, Malba V, Bernhardt A, Evans L, Harvey C, Chinn SC, Maxwell RS, Reimer J. J Magn Reson 2007;189:121–129. [PubMed: 17897853]
173. Adams KL, Klunder G, Demas V, Malba V, Bernhardt A, Evan L, Harvey C, Maxwell R, Herberg JL. Diffusion Fundamentals 2009;10:6.1–6.4.
174. Korir A, Larive C. Anal Bioanal Chem 2007;388:1707–1716. [PubMed: 17607565]
175. Eldridge SL, Almeida VK, Korir AK, Larive CK. Anal Chem 2007;79:8446–8453. [PubMed: 17929948]

176. Trumbull JD, Glasgow IK, Beebe DJ, Magin RL. IEEE Trans Biomed Eng 2000;47:3–7. [PubMed: 10646271]
177. Bednarek E, Bocian W, Michalska K. J Chromatogr A 2008;1193:164–171. [PubMed: 18440540]
178. Garcia-Perez I, Couto Alves A, Angulo S, Li JV, Utzinger J, Ebbels TMD, Legido-Quigley C, Nicholson JK, Holmes E, Barbas C. Anal Chem 2009;82:203–210. [PubMed: 19961175]
179. Keire DA, Trehy ML, Reepmeyer JC, Kolinski RE, Ye W, Dunn J, Westenberger BJ, Buhse LF. J Pharm Biomed Anal 2010;51:921–926. [PubMed: 19959313]
180. Kühnle M, Holtin K, Albert K. J Sep Sci 2009;32:719–726. [PubMed: 19278003]
181. Pertti JV, James PL. Electrophoresis 2006;27:1797–1810. [PubMed: 16645944]
182. Xiong B, Miao X, Zhou X, Deng Y, Zhou P, Hu J. J Chromatogr A 2008;1209:260–266. [PubMed: 18829035]
183. Li F, Wang D-D, Yan X-P, Lin J-M, Su R-G. Electrophoresis 2005;26:2261–2268. [PubMed: 15832297]
184. Pitois A, Heras LAdL, Betti M. Int J Mass Spectrom 2008;270:118–126.
185. Yin X-B, Li Y, Yan X-P. TrAC Trends in Anal Chem 2008;27:554–565.
186. Li Y, Jiang Y, Yan X-P. Anal Chem 2006;78:6115–6120. [PubMed: 16944892]
187. Whelan RJ, Zare RN. Anal Chem 2003;75:1542–1547. [PubMed: 12659220]
188. Inman W, Domansky K, Serdy J, Owens B, Trumper D, Griffith LG. J Micromech Microeng 2007;17:891.
189. Zhang C, Xing D, Li Y. Biotechnol Adv 2007;25:483–514. [PubMed: 17601695]
190. Ryu W, Huang Z, Prinz FB, Goodman SB, Fasching R. J Controlled Release 2007;124:98–105.
191. Mora MF, Garcia CD. Electrophoresis 2007;28:1197–1203. [PubMed: 17366482]
192. Piyasena ME, Lopez GP, Petsev DN. Sens Actuators, B 2006;113:461–467.
193. Chang ST, Paunov VN, Petsev DN, Velev OD. Nat Mater 2007;6:235–240. [PubMed: 17293850]
194. Yairi M, Richter C. Sens Actuators, A 2007;137:350–356.
195. Xu L, Dong X-Y, Sun Y. J Chromatogr A 2009;1216:6071–6076. [PubMed: 19576588]
196. Joo S, Chung TD, Kim HC. Sens Actuators, B 2007;123:1161–1168.
197. Li B, Jiang L, Wang Q, Qin J, Lin B. Electrophoresis 2008;29:4906–4913. [PubMed: 19130570]
198. Ducrée J, Haeberle S, Lutz S, Pausch S, Stetten Fv, Zengerle R. J Micromech Microeng 2007;17:S103.
199. Kim J, Kido H, Rangel RH, Madou MJ. Sens Actuators, B 2008;128:613–621.
200. Yoo J-C, La G-S, Kang CJ, Kim Y-S. Curr Appl Phys 2008;8:692–695.
201. Pappas TJ, Holland LA. Sens Actuators, B 2008;128:427–434.
202. Xu W, Wu LL, Zhang Y, Xue H, Li G-P, Bachman M. Sens Actuators, B 2009;142:355–361.
203. Leslie DC, Easley CJ, Seker E, Karlinsey JM, Utz M, Begley MR, Landers JP. Nat Phys 2009;5:231–235.
204. Jullien MC, Ching MJTM, Cohen C, Menetrier L, Tabeling P. Phys Fluids 2009;21:072001–072006.
205. Jean-Christophe G, et al. New J Phys 2009;11:075027.
206. Steinbock LJ, Stober G, Keyser UF. Biosens Bioelectron 2009;24:2423–2427. [PubMed: 19171475]
207. Sajonz P, Schafer W, Gong X, Shultz S, Rosner T, Welch CJ. J Chromatogr A 2007;1145:149–154. [PubMed: 17300788]
208. Ng SH, Wang ZF, de Rooij NF. Microelectron Eng 2009;86:1354–1357.
209. Sahlin E. J Chromatogr A 2007;1154:454–459. [PubMed: 17459399]
210. Culbertson CT, Tugnawat Y, Meyer AR, Roman GT, Ramsey JM, Gonda SR. Anal Chem 2005;77:7933–7940. [PubMed: 16351140]
211. Skelley AM, Scherer JR, Aubrey AD, Grover WH, Ivester RHC, Ehrenfreund P, Grunthaner FJ, Bada JL, Mathies RA. Proc Nat Acad Sci USA 2005;102:1041–1046. [PubMed: 15657130]
212. Biller, JE.; Herlihy, WC.; Biemann, K. Computer-Assisted Structure Elucidation. AMERICAN CHEMICAL SOCIETY; WASHINGTON, D. C.: 1977. p. 18-25.

213. Navarro-Gonzalez R, Navarro KF, Rosa Jdl, Iniguez E, Molina P, Miranda LD, Morales P, Cienfuegos E, Coll P, Raulin F, Amils R, McKay CP. Proc Nat Acad Sci USA 2006;103:16089–16094. [PubMed: 17060639]

214. Skelley AM, Cleaves HJ, Jayarajah CN, Bada JL, Mathies RA. Astrobiology 2006;6:824–837. [PubMed: 17155883]

215. Jayarajah CN, Skelley AM, Fortner AD, Mathies RA. Anal Chem 2007;79:8162–8169. [PubMed: 17892274]

216. Stockton AM, Chiesl TN, Scherer JR, Mathies RA. Anal Chem 2008;81:790–796. [PubMed: 19072718]

217. Stockton AM, Chiesl TN, Lowenstein TK, Amashukeli X, Grunthaner F, Mathies RA. Astrobiology 2009;9:823–831. [PubMed: 19968460]

218. Benhabib M, Chiesl TN, Stockton AM, Scherer JR, Mathies RA. Anal Chem 2010;82:2372–2379. [PubMed: 20151682]

219. Seiman A, Martin J, Vaher M, Kaljurand M. Electrophoresis 2009;30:507–514. [PubMed: 19145598]

220. Easley CJ, Karlinsey JM, Bienvenue JM, Legendre LA, Roper MG, Feldman SH, Hughes MA, Hewlett EL, Merkel TJ, Ferrance JP, Landers JP. Proc Nat Acad Sci USA 2006;103:19272–19277. [PubMed: 17159153]

221. Kaigala GV, Hoang VN, Stickel A, Lauzon J, Manage D, Pilarski LM, Backhouse CJ. Analyst 2008;133:331–338. [PubMed: 18299747]

222. Blazej RG, Kumaresan P, Mathies RA. Proc Nat Acad Sci USA 2006;103:7240–7245. [PubMed: 16648246]

223. Shi Y, Simpson PC, Scherer JR, Wexler D, Skibola C, Smith MT, Mathies RA. Anal Chem 1999;71:5354–5361. [PubMed: 10596215]

224. Liu CN, Toriello NM, Mathies RA. Anal Chem 2006;78:5474–5479. [PubMed: 16878885]

225. Toriello NM, Liu CN, Mathies RA. Anal Chem 2006;78:7997–8003. [PubMed: 17134132]

226. Liu P, Seo TS, Beyor N, Shin K-J, Scherer JR, Mathies RA. Anal Chem 2007;79:1881–1889. [PubMed: 17269794]

227. Rech I, Cova S, Restelli A, Ghioni M, Chiari M, Cretich M. Electrophoresis 2006;27:3797–3804. [PubMed: 17031786]

228. Rech I, Marangoni S, Gulinatti A, Ghioni M, Cova S. Sens Actuators, B 2010;143:583–589.

229. Berg C, Valdez DC, Bergeron P, Mora MF, Garcia CD, Ayon A. Electrophoresis 2008:4914–4921. [PubMed: 19130571]

230. Ryvolová M, Macka M, Preisler J. TrAC, Trends Anal Chem 2010;29:339–353.

231. Cifuentes A, Bernal JL, Diez-Masa JC. Anal Chem 1997;69:4271–4274.

232. Jacquier JC, Desbene PL. J Chromatogr A 1995;718:167–175.

233. Lin C-E. J Chromatogr A 2004;1037:467–478. [PubMed: 15214683]

234. Lin C-E, Wang T-Z, Chiu T-C, Hsueh C-C. J High Resolut Chromatogr 1999;22:265–270.

235. Stanley FE, Warner AM, Schneiderman E, Stalcup AM. J Chromatogr A 2009;1216:8431–8434. [PubMed: 19836753]

236. François Y, Zhang K, Varenne A, Gareil P. Anal Chim Acta 2006;562:164–170.

237. Østergaard J, Jensen H. Anal Chem 2009;81:8644–8648. [PubMed: 19775166]

238. Bharadwaj R, Park CC, Kazakova I, Xu H, Paschkewitz JS. Anal Chem 2007;80:129–134. [PubMed: 18044846]

239. Yan W, Colyer CL. J Chromatogr A 2006;1135:115–121. [PubMed: 17014857]

240. d'Orlyé F, Varenne A, Gareil P. J Chromatogr A 2008;1204:226–232. [PubMed: 18718601]

241. Li Y-Q, Wang H-Q, Wang J-H, Guan L-Y, Liu B-F, Zhao Y-D, Chen H. Anal Chim Acta 2009;647:219–225. [PubMed: 19591709]

242. Glynn JR Jr, Belongia BM, Arnold RG, Ogden KL, Baygents JC. Appl Environ Microbiol 1998;64:2572–2577. [PubMed: 9647832]

243. Ahmadzadeh H, Dua R, Presley AD, Arriaga EA. J Chromatogr A 2005;1064:107–114. [PubMed: 15729825]

244. Kostal V, Arriaga EA. Electrophoresis 2008;29:2578–2586. [PubMed: 18576409]

245. Seiman A, Reijenga JC. Procedia Chemistry 2010;2:59–66.

246. Wang GR, Sas I, Jiang H, Janzen WP, Hodge CN. Electrophoresis 2008;29:1253–1263. [PubMed: 18297657]

247. de Jesus DP, Brito-Neto JGA, Richter EM, Angnes L, Gutz IGR, do Lago CL. Anal Chem 2005;77:607–614. [PubMed: 15649060]

248. Saito RM, Neves CA, Lopes FS, Blanes L, Brito-Neto JGA, do Lago CL. Anal Chem 2007;79:215–223. [PubMed: 17194142]

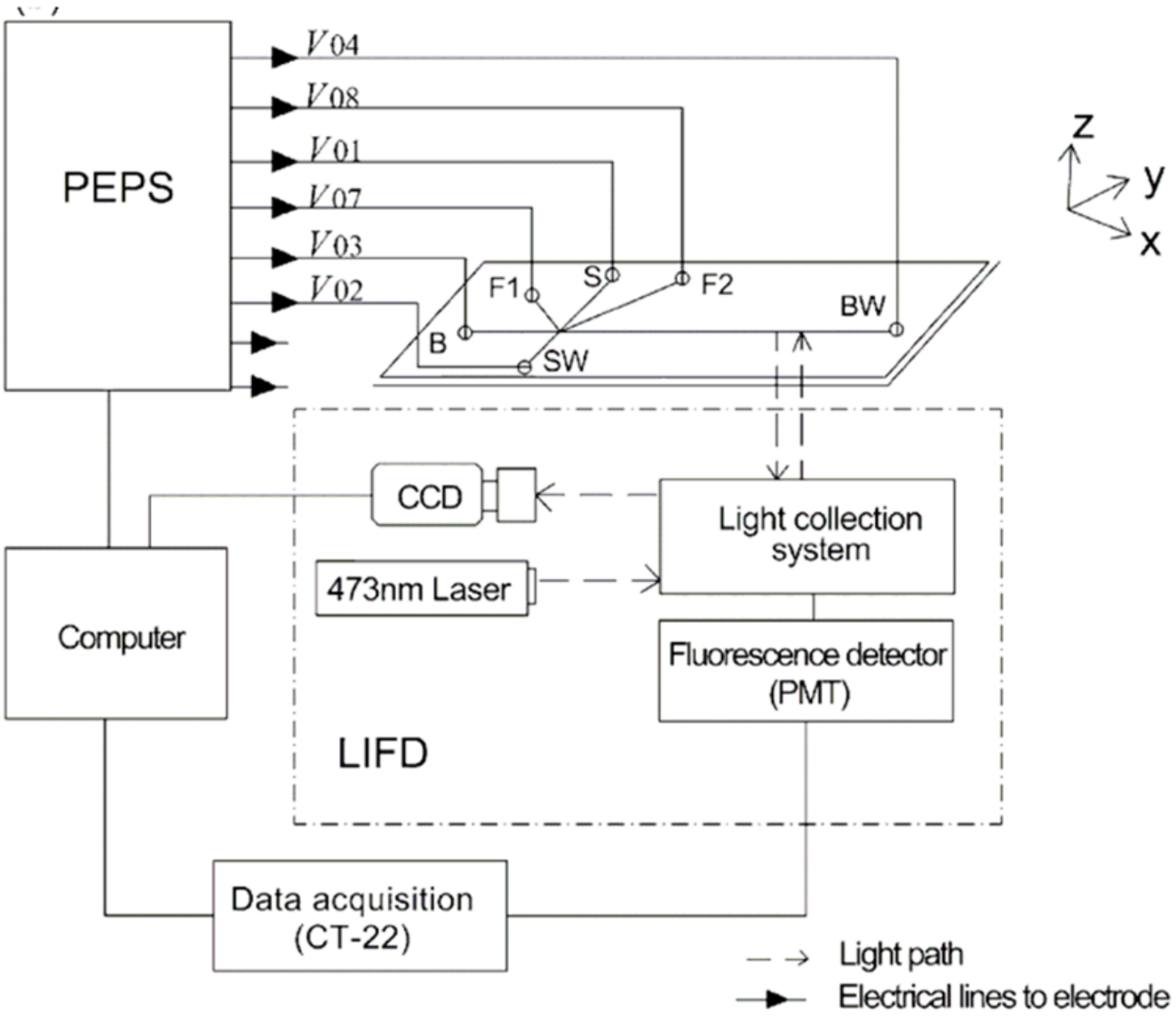

Figure 1.
Experimental set-up used to connect the PEPS with the microchip and the detection system. In this figure, each reservoir is addressed by an individual electrode. Adapted from reference [52].

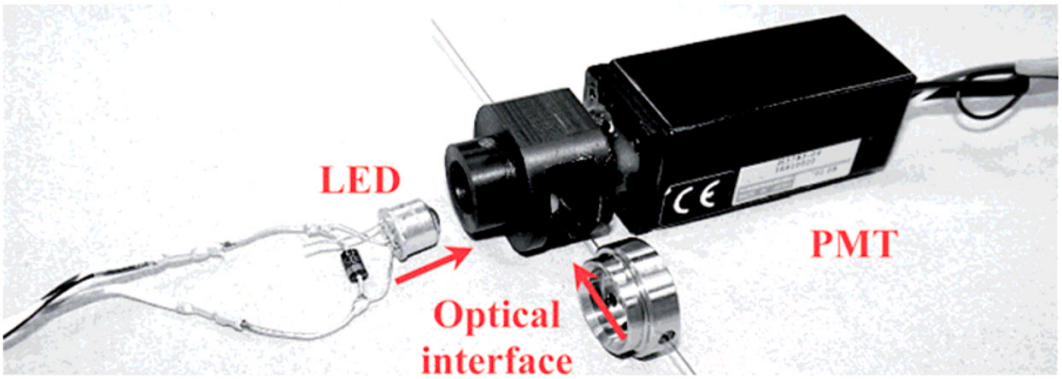

Figure 2.
Instrumental arrangement to perform optical detection using a deep-UV-LED. Adapted from reference [87].

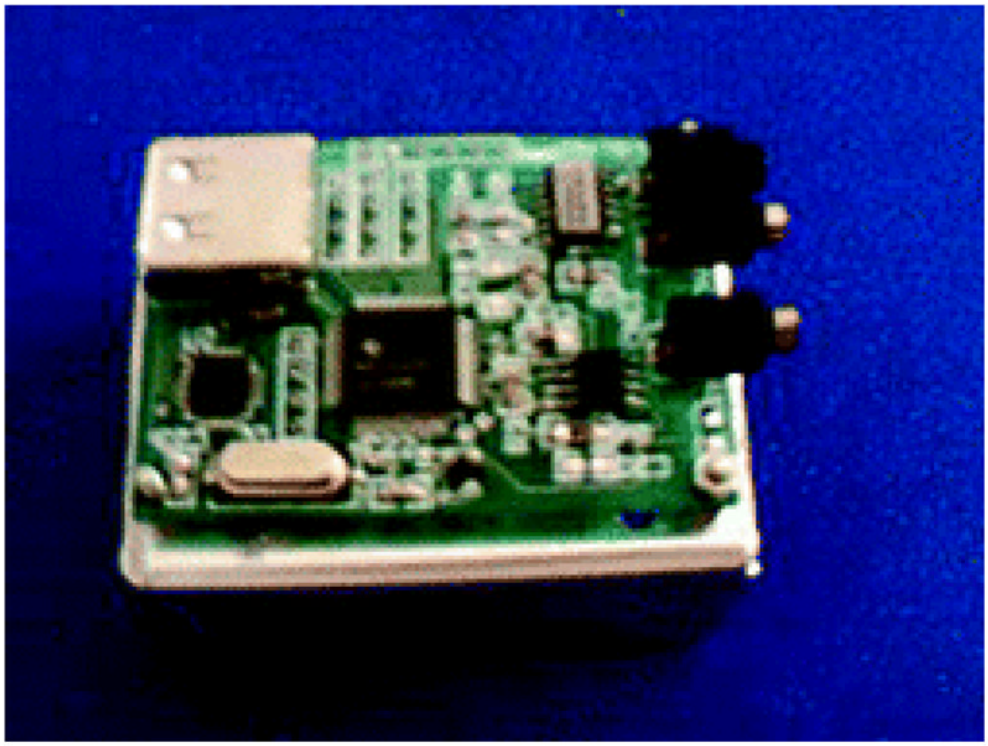

Figure 3.
Picture of the mini-ECD (3.6 × 5.0 cm) described in reference [51].

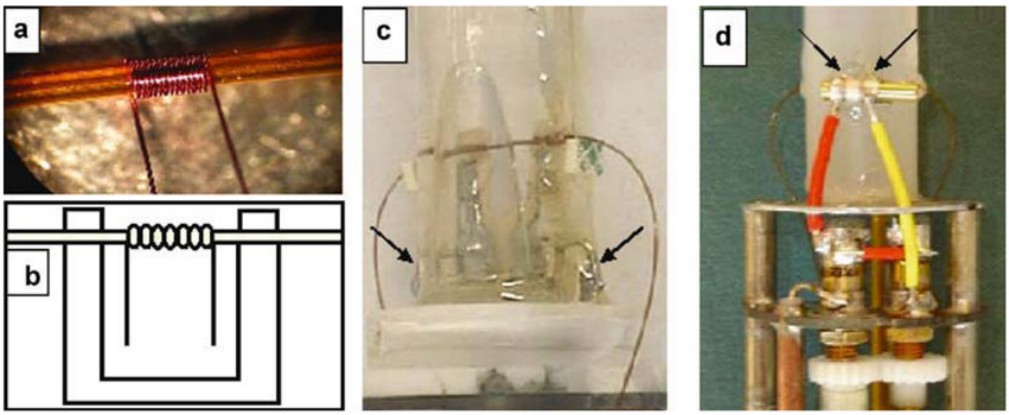

Figure 4.
a) Photo of the 14-turn coil used in the construction of the second-generation probe, b) illustration of how the microcoil is mounted on a plastic circuit board for mechanical support, photos of c) first- and d) second-generation probes showing some of the differences in design. The arrows indicate the points where the coil circuit was connected to the tuning capacitor. From reference [174].

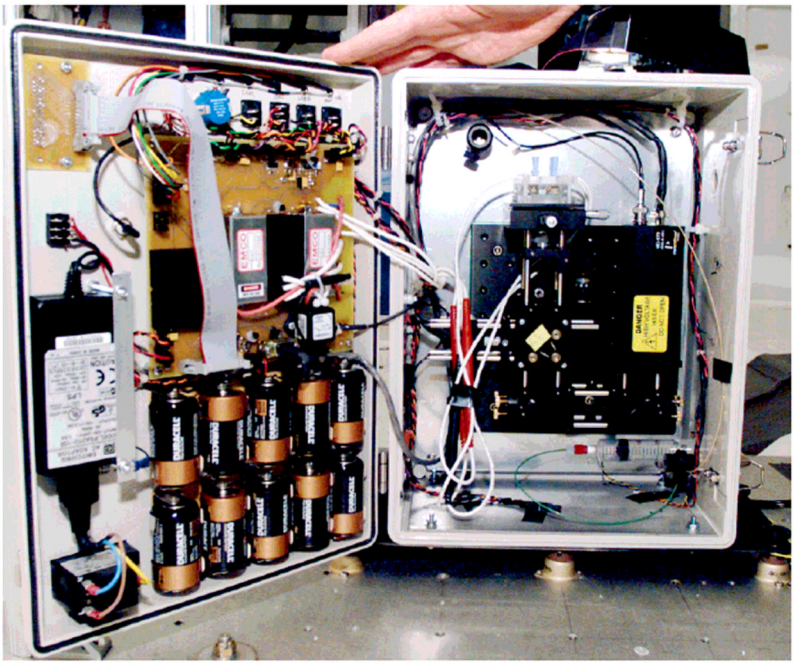

Figure 5.
Photograph of portable microfluidic device flown on NASA's microgravity research aircraft. From reference [210].

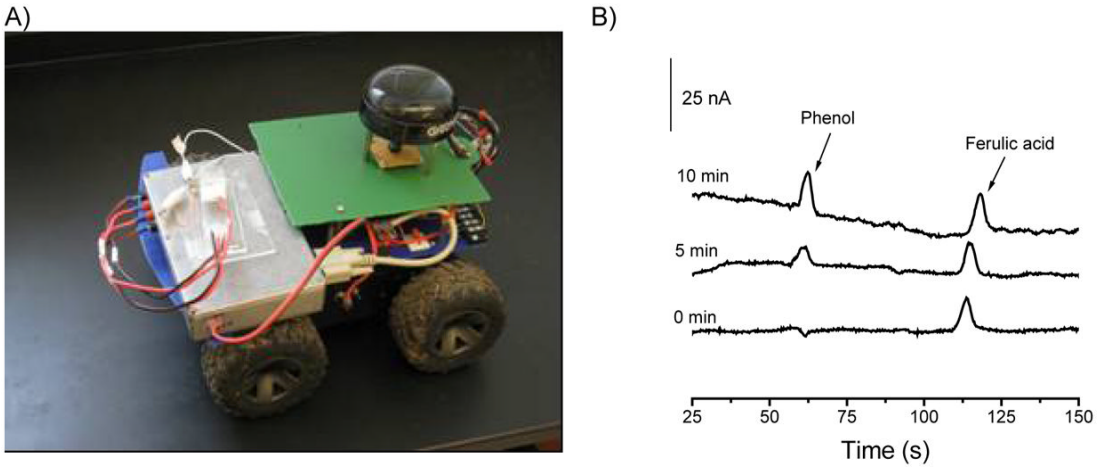

Figure 6.

Picture (left) of the assembled *Lab-on-a-Robot* containing HVPS, ECD, mobile platform, radiofrequency modem, compass, and GPS. Electropherograms (right) obtained wirelessly with the described *lab-on-a-robot*. Conditions: 5 mmol·L^{-1} phosphate buffer (pH=12.0), 1 mmol·L^{-1} sodium dodecyl sulfate, separation potential 1200 V, t_{inj}=7s, pulsed amperometric detection. Adapted from reference [229].

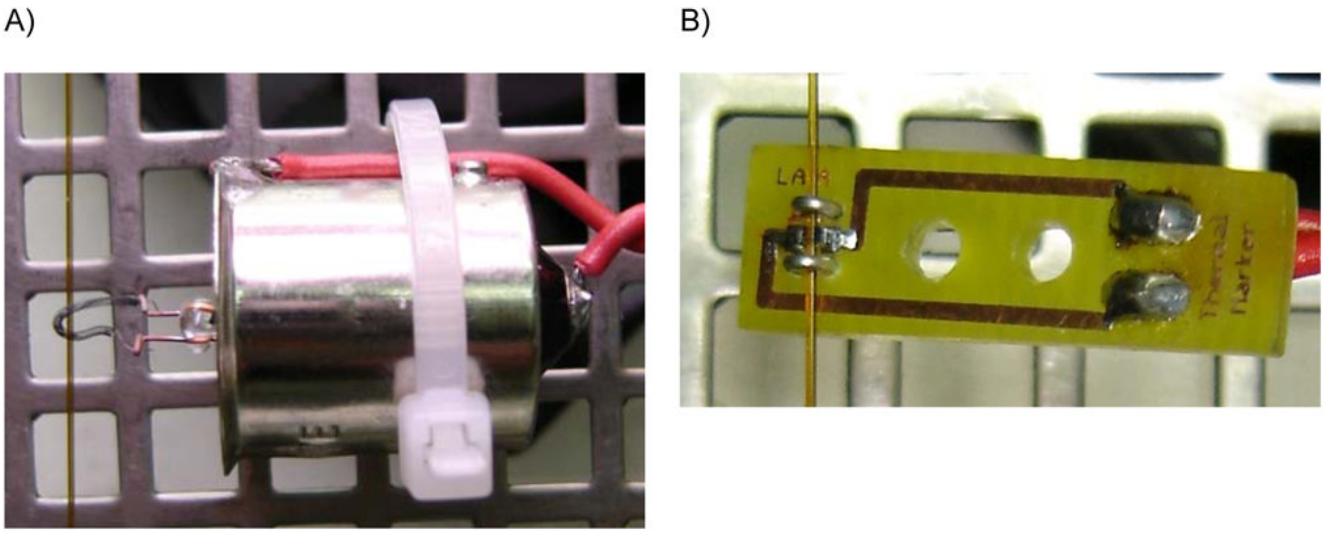

Figure 7.
Tungsten lamp (left) and SMD resistor (right) used to produce thermal markers. Both figures show the position of the silica capillary with respect to the heating elements. Adapted from reference [248].